IN SILICO STRUCTURAL ANALYSIS OF THE COMPLEX PSKR RECEPTOR LIKE KINASE, PAMP PHYTOSULFOKINE AND SERk1 CO-RECEPTOR

By

Hasnain Nizam Thakur
16136024

A thesis submitted to the Department of Mathematics and Natural Sciences in partial fulfillment of the requirements for the degree of
Bachelor of Science in Biotechnology

Mathematics and Natural Sciences
Brac University
February 2021

© 2021. Brac University
All rights reserved.

Declaration

It is hereby declared that

1. The thesis submitted is my own original work while completing degree at Brac University.
2. The thesis does not contain material previously published or written by a third party, except where this is appropriately cited through full and accurate referencing.
3. The thesis does not contain material which has been accepted, or submitted, for any other degree or diploma at a university or other institution.
4. I have acknowledged all main sources of help.

Student's Full Name & Signature:

Hasnain Nizam Thakur
16136024

Approval

The thesis titled “In silico structural analysis of the complex PSKR receptor like kinase, PAMP phytosulfokine and SERk1 co-receptor” submitted by Hasnain Nizam Thakur (16136024) of Spring, 2021 has been accepted as satisfactory in partial fulfillment of the requirement for the degree of Bachelor of Science on 2021.

Examining Committee:

Supervisor:
(Member)

_____

M H M Mubassir
Lecturer, Biotechnology Program
Department of Mathematics and Natural Sciences

Program Coordinator:
(Member)

_____

Iftekhar Bin Naser, PhD
Assistant Professor
Department of Mathematics and Natural Sciences

Departmental Head:
(Chair)

_____

Prof. Dr. A F M Yusuf Haider
Professor and Chairperson
Department of Mathematics and Natural Sciences

This page intentionally left blank.

Abstract

Plants often have to undergo pathogen invasions in nature. Nevertheless, as a result of proficient immune systems owned by the host plants, plant diseases seldom occur. In the process two separate recognition mechanisms identify pathogens, and one of them is known as pattern-triggered immunity (PTI) which plays an essential role in plant defense system. PRRs preliminarily conjoin to the pathogen-associated molecular patterns (PAMPs) in the case of a microbial incursion and then go on to ever further assigned co-receptor proteins to stimulate the defensive signal and optimize the immune response of the plant. While many plant PRRs have been found, only few have been thoroughly described and their structural specifications have been analyzed. In this analysis, the PSKR-Phytosulfokine-SERk1 (PDB ID: 4z64) complex crystallographic structure was simulated for 30 ns at several phases, as there were five different composites of the prime crystallographic composition. In order to obtain a synopsis of the interaction and immune responsiveness of PSKR against Phytosulfokine with the aid of co-receptor SERk1, 30ns of simulated trajectories were studied for each amalgamation. In addition, it was found here that from Phytosulfokine, Thr31 and Gln32 made a notable con tribution to the PSKR-Phytosulfokine complex development. It indicates that Phytosulfokine interacts predominantly with a β-strand from the PSKRR island domain and the development of an anti- β -sheet takes place in the process. Therefore, any alteration to the PAMP at these positions can be expected to be dramatically pernicious to the plant, resulting in the PRR failing its ability to detect the PAMP. As PSKR has been observed to play a key role in the plant defense mechanism of Arabidopsis thaliana, its theorized binding method with Phytosulfokine and SERk1 co-receptor can guide to draw a clearer picture of PTI's initial phases.

Dedication

This thesis is dedicated to my parents.

Acknowledgement

I would like to acknowledge everyone who played a role in my academic accomplishments.

I would like to express my sincere gratitude to **Prof. A F M Yusuf Haider**, Ph.D. Chairperson, Department of Mathematics and Natural Sciences, BRAC University, **Iftekhar Bin Naser, PhD** program Coordinator, Department of Mathematics and Natural Sciences, BRAC University for granting me permission to continue my research work in my desired field.

I would also like to extend my deepest gratitude to my supervisor **M H M Mubassir**, Lecturer, Biotechnology Program, Department of Mathematics and Natural Sciences who gave me the opportunity to work on this topic. Moreover, his insightful feedback and humble guidance pushed me to sharpen my thinking and brought my work to this level.

Thanks should also go to **Raghib Ishraq Alvy** whose expertise was invaluable in formulating this thesis work.

Table of Contents

List of Tables

List of Figures

List of Acronyms

AA	Amino Acid
ETI	Effector Triggered Immunity
GROMACS	Groningen Machine for Chemical Simulations
H-bonds	Hydrogen Bonds
LRR	Leucine Rich Repeat Domain
MD	Molecular Dynamics
PAMP	Pathogen Associated Molecular Pattern
PDB	Protein Data Bank
PRR	Pattern Recognition Receptor
PRR-RKs	Pattern Recognition Receptor like kinases
PTI	Pattern Triggered Immunity
Rg	Radius of Gyration
RMSD	Root Means Square Deviation
RMSF	Root Means Square Fluctuations
Thr	Threonine
Asp	Aspartic acid
Lys	Lysine
Gln	Glutamine

List of Symbols

Aº	Angstrom
K	Kelvin
nm	Nano meter
ns	Nano second
ps	Pico second

Chapter 1

Introduction

1.1Background Study

Lots of microbial pathogens are encompassed by plants, but somehow, they persist green. Plants do this by using their innate immune systems to recognize and demolish such pathogenic microorganisms. [1-4]

Miscellaneous life strategies are used by plant pathogens. Pathogenic microorganisms multiply in intercellular spaces (apoplast) after entering gas or water pores (stomata and hydathodes, separately) or gain access via wounds. Plants have no flexible defensive cells and a physically robust immune structure as compared to well evolved living thing (like a human being). Instead, they actually rely on each cell's genetic susceptibility and on the inherent signals that exude from the sources of invasion.[5]

The first of this mechanism is the vivid sensitive reflection of pathogen or microbe-associated molecular patterns (PAMPs or MAMPs) by pattern recognition receptors (PRRs) at the cellular surface of the plant. For instance, plants are assisted by pattern recognition receptors (PRR) 'FLS2 (flagellin sensitive 2)' a leucine-rich repeat receptor kinase (LRR-RK) placed within the plasma membrane to intercept bacterial flagellin. here the terminology 'PRR triggered immunity (PTI)' is used to assess biological responses to various MAMPs and flagellins.[2]

Effector Triggered Immunity (ETI) is another such immune response mechanism for plants whereby intracellular immune sensors are added and almost all of them are leucine-rich repeat (NBS-LRR) nucleotide-binding site proteins, that are designed for identification of detrimental effectors transmitted directly or indirectly.[6]

Henceforth, transmembrane pattern recognition receptors (PRRs) which respond in different steps for producing microbial or pathogen-associated molecular patterns (MAMPS or PAMPs), such as flagellin, are the first of the plant immune mechanism, and the following one functions within the cell by acknowledging all information's using the polymorphic NB-LRR protein items encoded by maximum R genes.[5, 7]

1.2 Research aims and objectives

The main aim of this research paper is to grasp pattern triggered immunity (PTI) in Arabidopsis thaliana, a model plant that utilizes the bioinformatics perspective for regulating the recognition of PSKR receptors. More precisely,

- Applying Molecular Dynamics (MD) Simulation to assess the reciprocal interaction among PRR- PSKR, PAMP-Phytosulfokine and Co-receptor SERK1.
- Co-Receptor SERK1s Participation in PTI guided by PSKR-Phytosulfokine complex structure.

1.3 Literature review

In this portion, fundamental description of pattern triggered immunity, the specified model plant as well as its morphology, several terminologies are assessed in accordance with pattern triggered immunity. At the end of this part, computational procedures and terminology analysis are also scrutinized.

1.3.1 *Arabidopsis thaliana*

The flowering plant, *Arabidopsis thaliana* has recently become an essential blueprint for the study of genes and their functional system.[8] In-plant biology, *Arabidopsis thaliana* is a common preference in these days for doing vast studies.[9] Latest Arabidopsis research indicates that this angiosperm is the right choice for most eukaryotes to do fundamental assessment of the functional and structural field of biology. There is a shared genetic lineage for most eukaryotic species and this was observed during the genome project.[10]

Obtaining a very tiny nuclear genome helps to make Arabidopsis a more appropriate guide for plant genomics.[11] This angiosperm is extremely resistant to ionizing radiation for the smaller genome, the interplay among radiation susceptibility and plant DNA composition was portrayed approximately sixty years prior.[12, 13]

From the preceding discussion, the potential factors for making *Arabidopsis thaliana* an effective genome analysis model can be clearly grasped. Other than a small nuclear genome, it

does have a short generation period, a substantial number of offspring as well as, apparently, a small size.[8, 14-16]

1.3.2 Morphology of *Arabidopsis thaliana*

Entire life cycle of Arabidopsis thaliana, including all the seed germination, rosette forming, main stem bolting, flowering and initial seed maturation, takes approximately six weeks to finish. Upon reaching a scale such as 2 mm flower in length , plenty of it is quite small, self-pollination mechanism due to exposed bud, pollen can be transferred to the stigma exterior for crossing.[10]

Seedlings are prepared in the rosette plant at maturity seed length of 0.5 mm, which varies from 2 to 10 cm in diameter according to growing procedures. The leaves used for observing cellular division and morphogenesis are trichomes, thin unicellular hairs.[10]

This part of the mustard family (Cruciferae or Brassicaceae) needs bolting after three weeks of transplanting. *Arabidopsis thaliana* flowers are composed of Silique creating a central gynoecium, pollen-bearing six stamens, four white petals containing inner whorls, and four green sepals containing outer whorls. then when the plants are 15-20 cm in height, approximately 5000 estimated seeds with quite a few hundred siliques are formed, that is indeed a developed plant.[10]

There seems to be no indication of a symbiotic connection with nitrogen-fixing microorganisms of the roots and the very composition to observe the culture.[10]

1.3.3 History of *Arabidopsis thaliana*

In plant biology literature in 1873, Alexander Braun proposed a mutant plant nearby Berlin, which was the very foremost non-taxonomic presentation of Arabidopsis.[17] Within that AGAMOUS gene, the mutation formed this is categorized these days as floral ABC regulators.[17, 18]

In 1907, Friedrich Laibach (1885-1967), a student of the Strasburger's laboratory, helped to make Arabidopsis properties easily accessible by presenting chromosome numbers of different plants. although the chromosomes of such plant are pretty short.[17, 19]

The presence of Arabidopsis was discovered again during the Russian expedition in 1935 to be used in genetics as well as cytogenetics instead of Drosophila because of the smaller number of chromosomes and flowering period is so prompt compared to others, however small volume and small pattern rendered it impossible at that time to distinguish chromosome pairs.[17, 20, 21]

Arabidopsis again appeared in 1943 when Laibach revealed that it has a limited generation span, ability to crossing, greater chance of mutagenesis, procreation, and so on characteristics that made it a blueprint for genetic model.[17, 22]

In plant biological research, molecular genetics and physiology, the revolution of the 1980s made comprehensive Arabidopsis' recognition as a model plant. Around that period, there were some proposals for models at plants that prefer petunia for its flexibility of transformation and abundance of haploid lines, tomatoes for mutant accessibility. However, in 1975, George Re'dei suggested Arabidopsis as a model plant for the discovery of auxotrophic mutation, and later it was highlighted in an article of the Annual Review of Genetics, which brought attention of the Cloners of molecules and aspiring geneticists.[17, 23]

In the summer of 2001, the 11th International Conference on Arabidopsis Research was conducted, in which the participation of about 1000 people contributed to the comprehensive acknowledgement of this experimental model system plant. This model genetic system has brought some kind of convergence of molecular and classical genetics in plant science through plant growth, physiology and pathology. Thus, for the very first time, information exchange and cellular activity techniques in plant life have become comprehensible.[17]

1.3.4 Pattern Triggered Immunity (PTI)

The very initial response of plant immune system is pattern triggered immunity (PTI), which is driven according to the stimulus of the microbe-associated or pathogen-associated molecular pattern (MAMPs or PAMPs) by pattern recognition receptor (PRRs).[1, 2, 5, 24, 25] Effector proteins have been acquired by adapted pathogens by evolution for suppressing PTI, which also is carried to the plant cell.[24, 26-28]

MAMPs (Microbe-Associated Molecular Patterns) DAMPs (damage Associated Molecular Patterns) emerged from the host at the time of invasion, and thus several forms of pathogens are generated. Cell surface-localized Pattern Recognition Receptors (PRRs) helps to detect

those pathogenic agents and after that these PRRs enable PTI for the immune system response.[29, 30]

Various microorganisms are successfully pulled off by PTI due to the conserved aspect of PAMPs (e.g., bacterial flagellin, fungal chitin). It therefore leads to basal immunity throughout the infection.[6]

PTI is useful for the majority of non-host pathogens by supplying a powerful and restrained immune response. PTI acts against adapted pathogens as a contributing factor to the basal inhibition, where effector proteins are often used to throw out PTI for host metabolism modulation which is called Effector Triggered Susceptibility (ETS).[30]

Present study has shown that PTI causes nutrient depletion to regulate microorganisms population, in addition to limiting pathogenic growth.[30, 31]

1.3.5 Effector Triggered Immunity (ETI)

The next plant immune system specializes in detecting effectors by supplementary receptors, classified as effector-triggered immunity (ETI). It is during the coevolution that these receptors are acquired.[5, 24, 32]

A Resistance (R) gene product within the plant cell, in ETI, detects the pathogen's effector protein(s) of the pathogen. Nucleotide-binding leucine-rich repeat (NB-LRR) proteins contain almost all of the R genes. ETI begins as these NB-LRR proteins recognize an effector. NB-LRR's method of recognition of effectors relies on the outcomes of their activity.[5, 24, 33]

These effectors are generally the product of modified pathogens and their purpose is to modify the physiology of the host and make it contagiously compliant, however the recognition capability of the NB-LRR protein generates a nerve battle among both plants and their pathogens.[6]

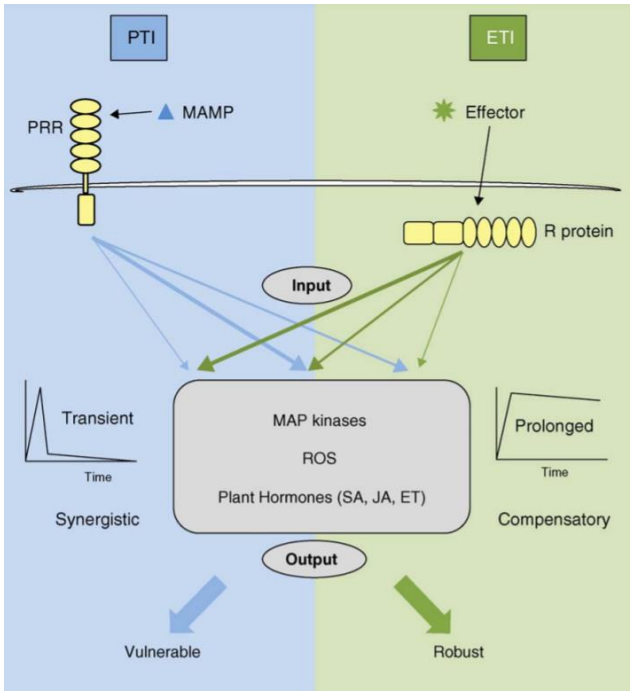

Fig 1.1: Signaling differences between PTI and ETI.[25]

1.3.6 Pattern Recognition Receptor (PRR)

Over 200 genes encoding leucine-rich repeat receptor-like kinases and also more than 1000 genes encoding putative secreted peptides have been detected in Arabidopsis Thaliana, which is trying to demonstrate that ligand-receptor peptide interactions are essential in plants for cell-to-cell correspondence.[34]

Phytosulfokine is recognized by receptor proteins belonging to the family of receptor-like kinases.[35] Two genes in *Arabidopsis thaliana* encrypt the leucine rich repeat (LRR) PSK receptor kinase.[36] The subfamily LRRX of the LRR receptor kinase family has indeed been authorized to PSKR1 and PSKR2.The vast family of leucine rich repeat receptor kinases (LRRRKs) with an extracellular LRR domain and a cytoplasmic kinase domain contains PSKR (KD). The three LRR-RKs' extracellular domains contain 21 LRRs each containing 24 amino acids. LRR 18 is disrupted by an island domain which is completely necessary for PSK foresight.[37]

Within the plasma membrane, the PSKR does seem to have a single helical transmembrane domain that anchors it. Widely predicted serine/threonine kinase depending on the 12 subdomains usually identified in this class of kinases is the cytoplasmic region of PSKR.[37]

PSK binding stimulates signaling upheld by PSKR1 binding Ca2+/CaM and kinase response, indicating that $PSKR1^{KD}$ is activated by ligand binding, as seen in well-researched RKs such as flagellin insensitive 2 (FLS2) and brassinosteroid insensitive 1 (BRI1). Latter two receptor kinases mediated signaling includes ligand-enhanced heterodimerization along with LRR-RK BAK1, a member of somatic embryogenesis receptor-like kinases (SERKs) that typically function with additional LRR-RKs as a coreceptor.[37]

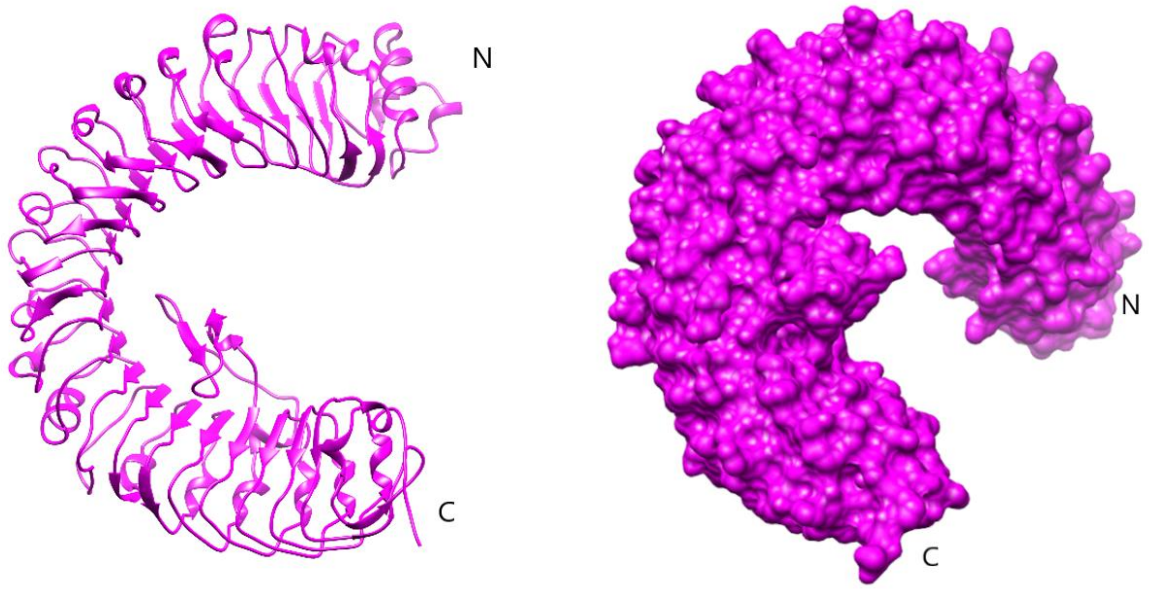

Fig1.2: Illustration of PSKR LRR in cartoon and surface structural view

1.3.7 Leucine-Rich Repeat Receptor-like Kinase

particular receptors serve to guide signals and detect foreign activity on the cell surface of living organisms; however, this technique is facilitated by receptor-like kinases (RLKs) with respect to plants. One amongst them as well as the largest family with two forms of domains is the Leucine-rich repeat RLK family. Such as, Extracellular domain (ECD) and Kinase domain (KD). The distinctions between ECD and KD are: ECD comes with a variety of LRR repeats that assist to detect tiny molecules, whole protein or peptides, while KD appears to

contain 12 subdomains which are effectively retained and folded into a three-dimensional two-lobed structure catalytic center. And these subdomains play a prominent part in the functioning of enzymes.[38, 39]

1.3.8 Pathogen Associated Molecular Pattern (PAMP)

Unique molecular patterns of microorganisms that perform the leading role of innate immunity in the plant model are known as pathogen-associated molecular patterns (PAMP).[40-43] The most probable specificities of understanding immensely retained molecules obtained independently through convergent evolution for various kingdoms.[43-45] In the initial step, host sensing PAMPs easily lead to activation of the protection mechanism by strengthening the cell wall by callose accumulation, generation of reactive oxygen species (ROS), etc. Afterwards the first level, these PAMP stimulated basic protection mechanisms can be hindered by virulence elements of comprehensive pathogens. Ultimately, to detect these virulence agents originating from the pathogen and their efficacy upon on host, developed resistance (R) proteins have been produced.[43, 46-48]

A hypersensitive response (HR) which constitutes of targeted cell death as well as acquisition of PAMP transformation emerges as a consequence of R protein-dependent sensing.[43, 49, 50]

1.3.9 Phytosulfokine (PSK)

As we know that, in regulating plant physiology, peptide signaling has a crucial function. Hence it is also known that, Phytosulfokine (PSK) is a disulfated secreted pentapeptide (Tyr (SO3H)-Ile-Tyr (SO3H)-Thr-Gln) with a widely recognized function in the augmentation and progression of plants. For its complete activity, PSK evolves by proteolytic cleavage of its descendant proteins with post-translational sulfation.[37] The PSK receptor was first recognized in Daucus carota (carrot) and also the corresponding DcPSKR gene is persisted between plants as well as Arabidopsis, that encodes two PSKR orthologues, PSKR1[51] and PSKR2 [52], yet PSK determination largely depends on PSKR1[37, 52]

The structures signify that PSK pretty much exclusively associates with a b-strand from PSKR's island domain, rendering an anti-b-sheet. The two PSK sulfate residuals inevitably link to

PSKR, influencing PSKR's acceptance of PSK. PSK attachment helps to increase PSKR heterodimerization with somatic embryogenesis receptor-like kinases (SERKs) along with the additional assistance of biochemical, structural and genetic data. Besides that, PSK is not precisely engaged in PSKR-SERK interlinkages, rather harmonizes the SERK interaction sphere of PSKR island.[37]

Fig 1.3: Cartoon and surface structural view of PSK

1.3.10 SOMATIC EMBRYOGENESIS RECEPTOR-LIKE KINASE1 (SERK1)

SOMATIC EMBRAYOGENESIS RECEPTORLIKE KINASE1 (SERK1), an LRR-RLK that functions to just trace embryogenic cell construction in culture and is demonstrated simultaneously in male and female gametophytes in ovule primordia. Its stimulation is prevalent in all organ vascular tissue, although it depicts a dynamic pattern in sporophytic tissues. In Arabidopsis plants, SERK1 preterm expression does not occur in a precise phenotype, yet maximizes somatic embryos in culture. It is part of a small family of five associated RLKs, that do have a baseline area of the Ser-Pro-rich juxta membrane. [53-56]

SERK1 aligns with KINASE-ASSOCIATED PROTEIN of PHOSPHATASE (KAPP), that always performs a Act in reinforcing receptors. There is hardly any morphological phenotype for Knockout alleles of SERK1, yet again the combined effect more with the serk2 void mutant culminated in comprehensive male-sterile plant species. [53-58]

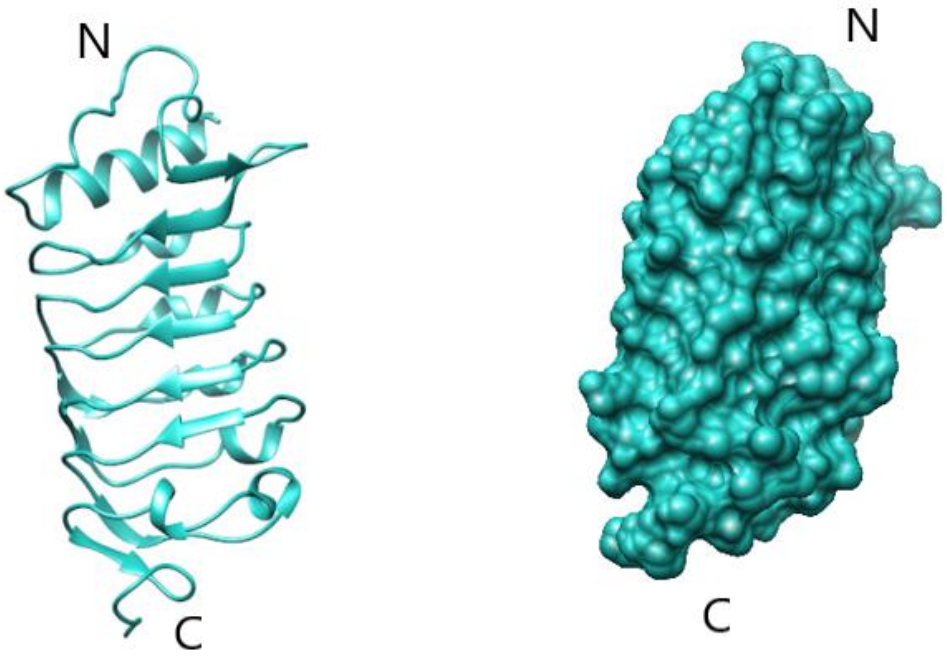

Fig 1.4: Co-receptor SERk1's surface and cartoon structural representation

1.3.11 Activation of SERK1 with PRRs

PSKR1 interaction with the N-terminal side of SERK1LRR is predominantly intervened by van der Waals links. Focused at this interaction is SERK1^{Thr59} that firmly wrap opposed to PSKR1^{Leu516} and PSKR1^{Tyr518}. assemble of SERK1^{Phe61} against PSKR1^{Pro525} further toughens up the fundamental interaction around this interface. More comprehensive PSKR1LRR–SERK1LRR interactions occur from connections of the residues PSKR1^{Phe596}, PSKR1^{Ser598} and PSKR1^{Thr619} from one lateral side of PSKR1 with the inner surface of SERK1LRR. The PSKR1LRR–SERK1LRR interactions are extremely retained in the PSK–DcPSKRLRR–SERK2LRR complex.[37]

Co-expression of unabridged Flag- linked PSKR1 (PSKR1–Flag) with haemagglutinin (HA)-conjugated SERKs leading to rupture of Arabidopsis protoplasts promptly. Therefore, the method utilized a KD condensed PSKR1 (PSKR1(DKD))–Flag and SERK1/SERK2/BAK1–HA for coexpression in protoplasts.[35] Co-immunoprecipitation (Co-IP) assays demonstrated that PSKR1(DKD) interacted with SERK1, SERK2 or BAK1 in protoplasts even in the dearth of PSK, perhaps ensuing from the endogenous PSK or their essential interaction, as observed for the BRI1–BAK1 interaction. Significantly, the PSKR1(DKD)–SERK interactions were considerably further in the PSK-treated protoplasts. Corresponding outcomes were also found in Arabidopsis co-expressing PSKR1 and BAK1, SERK1 or SERK2.[37, 59]

1.3.12 PSKR-phytosulfokine complex

The design of the protein complex was collected from the "Protein Data Bank" (PDB code: 4z64). we know already that PSK adopts a β-strand configuration, shaping an anti-parallel β -sheet with the $PSKR1^{ID.}$ Moreover, the hydrogen bonds across the β -sheet, $PSKR1^{Ser370}$, $PSKR1^{Ser372}$, $PSKR1^{Thr398}$ and $PSKR1^{Asp445}$ from the inner side of the helical structure also form hydrogen bonds with the prime chain of PSK.[37, 59]

In addition to that, $PSKR1^{Arg300}$ and $PSKR1^{Asn346}$ form hydrogen bonds along with free carboxyl group of PSK^{Gln5}, whilst $PSKR1^{Phe506}$ firmly packs against PSK^{Gln5} and PSK^{Tyr3}. The two sulfate residuals provide to PSK–$PSKR1^{LRR}$ interactions through both hydrogen bonds including $PSKR1^{Lys508}$ and $PSKR1^{Asn424}$ and van der Waals packing including $PSKR1^{Leu399}$, $PSKR1^{Trp448}$ and $PSKR1^{Lys508}$.[35] The PSK-interacting residual of PSKR1 are highly preserved in DcPSKR and PSKR2, Seems to indicate that the three PSKRs are preserved in PSK recognition. certainly, the structure of PSK–$DcPSKR^{LRR}$ is nearly alike to that of PSK–$PSKR1^{LRR}$ with a r.m.s.d. (root mean square deviation) of 1.45 A˚.[37, 52, 59]

Supplementary assisting the sulfate group-mediated PSK–$DcPSKR^{LRR}$ reciprocities, microscale thermophoresis (MST) revealed that PSK demonstrated a greater binding connection with $DcPSKR^{LRR}$ than the desulfated PSK (dPSK), Consenting the observation that dPSK encourages root expansion of Arabidopsis plants but with a lower activity than PSK.[35, 37, 52, 59]

1.3.13 Computation approach for Molecular Dynamics (MD) simulation

Simulating the movement patterns of an approach known theoretically as Molecular Dynamics of distinct particles. As a core idea, the mechanism is small like just an atom and a diatomic particle performs a relatively large chemical reaction more like solar system.[60, 61] Perception of the interaction efficiency of the components is important in order to develop a molecular dynamics simulation.[61]

Unique particle motions are utilized as a function of time actually to elicit precise data and to adapt to the parameters of simulations of a model structure. Throughout the domain of macromolecular science, three distinct forms of simulation methods exist mainly. The initial one is focusing on a sample selection of standard position for the design, this helps to describe mechanisms with the knowledge obtained from research on theoretical or veritable processes. The secondary approach includes structural as well as motional attributes and the values of thermodynamic parameters to define the mechanism in balance. The exact dynamics was studied by the third approach, where the key consideration is the motion and progression of individual particles throughout time.[62]

system accessibility as well as computing capacity must always be needed to perform practical works on biological macromolecules through molecular dynamics (MD) simulation. In former days, the simulation was less than 10 ps in duration, but the current scenario demonstrates that 1000 times lengthier simulations of same sizes are mostly conducted within half of the time than it was before. Other than just time, the computing power with which several simulation items can be done is another significant fact of simulation. The most commonly applied systems are CHARMM20 AMBER21 and GROMOS22.[62-65] It can often be difficult to get the right outcome in the research lab for the lack of intense and regulated temperature and pressure where such problem is solved by computer simulations.[66]

1.3.14 Protein Interactions Calculator (PIC)

Protein consistency on the basis of origin and function of protein atomic interaction research in their tertiary constructions is essential for a greater grasp of sequence configuration correlations. Remote homology identification methods, protein folding identification, protein

structure comparisons, as well as protein information modeling are utilized to recognize sidechain interactions. Such insight sometimes tends to help to do location-based mutagenesis research and comprehend the residue retention of homologous proteins.[67-75] Furthermore, regions of intense understanding are the interaction amongst subunits of multimeric proteins and sometimes between interacting protein modules.[74, 76-80] Features of sidechain sidechain correlations around protein components provide an illustration of the evolutionary persistence of protein-protein relationships.[74, 81-83] The Protein Interactions Calculator (PIC) is an internet platform that analyzes various sorts of interactions in protein tertiary arrangements as well as protein clusters. It also has a solvent accessibility calculator for demonstrating the visible motifs from the interacting ones. Apparently, the PIC server facilitates the protein structure's atomic projection collection in the conventional PDB or Protein Data Bank format.[74]

1.3.15 MM-PBSA

Molecular mechanical forces together with the Poisson Boltzmann and surface area continuum solvation (MM/PBSA) system are utilized to assess the free energy of the attachment of delicate ligands to biological polymers. Generally, this strategy relies upon molecular dynamics modeling of the structure of the receptor ligand-binding site. For drugs designing and protein structure assessment, free energy measurement is used.[84-86] MM-PBSA precisely blends in order to measure ligand binding predispositions, molecular dynamics and continuum solvent systems. The MMPBSA process has been constructed and kept up to date in accordance with the form usability.[85, 87-89] The scheme is utilized for the configuration of proteins, correlations among proteins, stabilization of conformers and rescoring. MM refers to molecular mechanics here, PB means Poisson-Boltzmann and then SA for surface area. Throughout this procedure, three distinct energy parameters are presented as yield as per their standards.[85, 88, 90-96]

1.3.16 Solvent accessible surface area (SASA)

Heretofore developed, solvent accessible surface area plotted out by the center of a probe territory depicting a solvent substance spread out over surface of the molecule of concern. This discovery used as a strategy for targeting the protein folding issue. It is not adequate for further

research findings to only accurately measure a quantity region, so that another method has been proposed. In the process Rather than disrupting the surface of the atoms that are open to the van der Waals Surface Interaction It creates a connection across a channel of concave and saddle-shaped surfaces. [97-99]Later, the procedure by which a small problem is solved is re-developed. If the probe sphere is omitted and van der Waals overlapping also is not experienced, then how can SASA of the molecule be measured? Through developing algorithms for measuring interaction as well as reentrant areas, and even the solvent accessible area that helps measure certain molecules' SASA. [97, 100-102]

1.3.17 Hydrogen Bond

The hydrogen bond is perhaps the most significant interatomic interaction in protein folding. The normal intermolecular hydrogen bond energy is very small compared to covalent bond; however, their large number of affiliations has a huge effect on protein folding in another manner, it regulates the folding process, yet their position is mainly preserved for hydrophobic interaction. [103-106]

Almost all of the protein hydrogen bonds are NH to CO main chains, and bonds among mainchains and side chains form a cluster across the helices caps. Inability to establish hydrogen bonds of main chain NH or CO groups is quite unlikely. [106]

Chapter 2

Materials and Methods

Procedures followed for the evaluation of interaction between PSKR-Phytosulfokine-SERK1 are listed in this section. Various kinds of open-source programming software and databases have been used for data analysis. Such as, GROMACS 5.0, MM-PBSA, RCSB Protein Data Bank, Protein Interactions Calculator (PIC), XmGrace, Chimera, and so on. For the open-source platform, all the software is constructed and the validation procedures are carried out for implementation on the Linux-based Ubuntu platform.

2.1 Molecular dynamics simulation of PSKR LRR, PAMP Phytosulfokine and Co-Receptor SERk1

Initially, the first amalgamation of the receptor ectodomain PSKR with PAMP Phytosulfokine and Co-Receptor SERk1 (PDB code: 4z64) was retrieved from the web server of the Protein Data Bank. The file was downloaded using the format '.pdb'. Then In a text editor, the PDB file was organized and updated by retaining all the protein residues inside. After storing the document, PIC data was procured in accordance with the search section for protein-protein interaction. Afterward, the PDB file was sent to the GROMACS software framework for molecular dynamics (MD) simulation. [107] For this simulation, GROMOS 54a7 unified force field was chosen. The scheme was then solvated, neutralized, energy reduced and stabilized. The protein complex was applied to a cubic box with a minimum distance of 1 Å during solvation, extending from the protein surface to the verge. The recently created box with the inner protein complex was solvated with the SPC water system. .[108]The process was nullified with the Genion function of GROMACS prior to actually switching to energy minimization. 1 ns NPT coordinates followed by 1 ns NVT parameters were matched during balancing while preserving a stable 1 atm pressure as well as 300 K temperature. The produced output file is 'md 0 1.gro'. By using GROMACS module, the gro file was converted from 'md 0 1.gro' to 'md 0 1.pdb'. In addition, except for remnants in the text editor, solutions were omitted and the save file was updated. In the context of protein-protein interaction data collection, the pdb file was utilized for PIC.

2.2 Analysis of binding mode of PSKR LRR with PAMP Phytosulfokine and Co-receptor SERk1

Intermolecular correlations among PSKR LRR, Phytosulfokine and SERk1 co-receptor were formulated in the complex utilizing Chimera, a molecular representation system. By using protein interactions calculator (PIC) tool, H-bonds, hydrophobic interactions, ionic interactions, aromatic interactions and cation-Pi interactions were measured. Again, for structural complex, before and after the simulation, all forms of testing were performed. Moreover, by using g_mmpbsa system, binding free energy results were calculated.

Chapter 3

Result and Discussion

Interrelationships among PSKR LRR with PAMP Phytosulfokine and co-receptor SERk1 were discussed in this segment, as well as graphs and figures were also displayed. In the final section of this report, the molecular interactions between the three complex proteins pre and post MD simulation, the molecular interactions among PSKR-Phytosulfokine pre and post MD simulation, and the molecular interactions among PSKR-SERk1 were computed and demonstrated. The MM/PBSA approach was adopted and extensively demonstrated with relevant figures in this portion for detailed study of interlinkages.

3.1 MM/PBSA

Table 3.1.1: The predicted binding free energies and the individual energy components for the studied systems (kJ/mol)

Complex	ΔE_{vdw} [a]	ΔE_{elec} [b]	ΔE_{polar} [c]	ΔE_{sasa} [d]	ΔE_{bind} [e]
PSKR+Phytosulfokine	-133.807 ± 16.592	-306.852 ± 78.825	505.852 ± 121.976	-18.462±1.670	46.731 ±43.134
PSKR+SERK1	-364.937 ±41.888	-625.297 ±107.510	687.465 ±150.459	-45.069 ±7.465	-347.837 ± 125.931
Phytosulfokine+SERK1	-0.700± 0.222	-9.573 ± 4.453	4.899±58.227	-0.219 ± 2.754	-5.593±58.248
PSKR+SERK1	-495.662 ± 37.067	-685.959 ± 97.802	797.877 ± 148.463	-56.786 ± 7.040	-440.530 ±109.154
PSKR+Phytosulfokine	-104.858 ±20.188	-421.876 ± 103.287	548.977 ± 132.562	-16.156 ± 3.108	6.087 ± 38.811
Phytosulfokine+SERK1	-38.112 ±18.765	-92.602 ± 37.513	105.706 ± 67.130	-6.762±3.116	-31.770 ±34.157

[a] Van der waals energy. [b] Electrostatic energy. [c] Polar solvation energy. [d] Solvent Accessible Surface Area (SASA) energy. [e] Binding Free energy. Every simulation is performed on 100ns where first three rows are from three protein complex.

Based on the calculation of MM/PBSA (Table 3.1.1), The binding energies procured among PSKR, phytosulfokine and SERK1 are -347.837 kJmol-1 and -5.593 kJmol-1 (when PSKR interacts with SERK1) and (when phytosulfokine interacts with SERK1). In addition, PSKR associates with SERK1 lacking phytosulfokine and has a binding energy of -440.530 kJmol-1, i.e., additional significant interaction. In the nonexistence and existence of SERK1, nevertheless, there really is no connection between PSKR and phytosulfokine the binding energies, since in that condition, are 46,731 kJmol-1 and 6,087 kJmol-1 accordingly. Upon on basis of this synopsis, this can accurately be indicated that there is a notable participation of the co-receptor SERK1 in the relationship between PSKR and phytosulfokine. In addition to adding, in terms of intermolecular Van Der Waals energy and electrostatic energy, highly favorable value can be noted for interacting between PSKR, phytosulfokine and SERK1. When phytosulfokine is present in the complex and when polar solving energy of PSKR and SERK1 is unavailable, PSKR readily engages with SERK1, but the contribution of Van Der Waals energy formulates complex interactions. There is also another interpretation that indicates different circumstances of PSKR interacting with phytosulfokine lacking SERK1, since it is found from intermolecular electrostatic energy that when SERK1 is present in the complex electrostatic energy, it is less beneficial for the PSKR and phytosulfokine complex, but if SERK1 is absent, it produces considerably lower electrostatic energy. Nevertheless, Co-Receptor SERK1 must be involved in the complex for the occurring interaction among PSKR and phytosulfokine so the presence of SERK1 helps interact with phytosulfokine by showing negligible binding affinity. In the exclusion of SERK1, enhancement of the polar solvation energy of PSKR and phytosulfokine enables the binding energy between these two proteins to be comparatively lower.

A divergent energy input is measured for the whole single residue for a detailed analysis. It is seen from this calculation that phytosulfokine Arg300, Arg327, Met507, Arg514, Glu529, Asp553, Glu574 from PSKR and Thr31, Gln32 play a key role in constituting MM energy for the interaction amongst themselves. Where MM energy, electrostatic energy and covalent bond are an amalgamation of Van Der Waals energy. When SERK1 is present in the Arg300, PSKR and Thr31 Met507 complex, phytosulfokine Gln32 displays relatively more non-polar energy than others, which suggests that these residues are accountable for the relationship between PSKR and phytosulfokine in van der Waals. None the less, at this phase, full electrostatic energy comes off. Without SERK1, there is negligible non-polar energy for PSKR's Arg300, Met507, whereas other mentioned PSKR and phytosulfokine residues provide higher

value than before. Furthermore, when PSKR interacts with SERK1, Arg30, Lys87, Arg109, Lys113, Lys158, Arg492, Lys547, Lys548, Lys599 are essential residues of PSKR. Lys113 and Lys599 only give marginal non-polar energy from such sources. From SERK1 Glu29, Asp31 and Asp42, respectively. Asp51, Glu68 and Glu80 are residues of essential significance. Glu68 from SERK1 alone has a lower non-polar value limit. Thus, van der Waals energy also works to establish mutual partnerships between PSKR and SERK1 alongside electrostatic energy. From (Table 3.1.2-3.1.7) PSKR's Arg300 reveals the uttermost binding free energy for phytosulfokine presence, which is -6.9089 ± 0.1261 kJmol-1 in the nature of SERK1 and -7.1805 ± 0.1176 kJmol-1 in the SERK1 insufficiency. In place of phytosulfokine Thr31 and Gln32, maximal binding free energy is indicated when dealing with PSKR, which is -3.8066 ± 0.1791 kJmol-1 and 2.1566 ± 0.7372 kJmol-1 in the presence of SERK1 and -14.8964 ± 0.2438 kJmol-1 and -17.4842 ± 0.8586 kJmol-1 in the lack of SERK1. Whichever approach, electrostatic interplay is more prominent than the contact with van der Waals. The referred remnants from PSKR and phytosulfokine play an equally important role in the graphical manner, while Arg300 of PSKR interacts very favorably with phytosulfokine whereas SERK1 is absent in the complex, but some remnants display beneficial interlinkages in the presence of SERK1. The phytosulfokine interaction of Thr31 is more conducive to the SERK1 aspect, however without SERk1, Gln32 provides favorable interaction. All residues have extra favorable status for PSKR and SERK1 interlinkages when phytosulfokine is present in the complex, yet SERK1's Asp42 and Glu80 are more favorable when phytosulfokine is absent in the complex.

From Protein Interaction Calculation (PIC) (Table 3.3.1-3.3.21) for PSKR as well as phytosulfokine interaction, just Thr31 from phytosulfokine display coordination in specific interactions after the computer simulation method is acknowledged as favorable from MM/PBSA analyses among these residues. In the presence and absence of SERK1 and protein-protein main chain side chain hydrogen bond interaction, Thr31 from phytosulfokine partakes in the protein-protein side chain side chain side chain hydrogen bond interaction whereas SERK1 is absent. For the PSKR and SERK1 complex, PSKR's Lys158 engages in ionic protein-protein interaction with SERK1 (Asp31) residues after simulation. Asp31 only from SERK1 contributes in ionic activity with PSKR residues whereas phytosulfokine is present and absent within the complex throughout the simulation process. In addition to an in-depth dissection of the energy contribution of each individual residual and with the guidance of Protein Interaction Calculation (PIC) details, various unique residues from all these three

proteins are revealed from the synopsis of MM/PBSA assessment that are responsible for interacting between PSKR, phytosulfokine and SERK1. For PSKR, Lys158 is the solely responsible residue for SERK1 interaction formulation. It supplies comparatively high MM energy side by side with other residues of PSKR from MM/PBSA. furthermore, this residue from PIC also participates in divergent ionic contact. Consequently, Lys158 from PSKR offers electrostatic energy with several other interactions to increase binding affinity with SERK1. Nevertheless, with respect to phytosulfokine, Gln32 generates more MM energy to engage in more interactions with PSKR Thr31. These two phytosulfokine residues are responsible for PSKR interaction build-up.

Asp31 and Glu68 from SERK1 are responsible for engaging with PSKR in favor of another scenario. Nonetheless, in the midst of these residues, in the whole percentage of measurement techniques, Asp31 is by far the most responsible. In the phytosulfokine company, -28,7104 kJmol-1 MM of energy derived from electrostatic energy and some subsidies for van der Waals energy and without phytosulfokine, -26,2942 kJmol-1 MM of energy derived from electrostatic energy and some subsidies for van der Waals energy. In comparison to the participation of other SERK1 residues, those two values are relatively higher. In addition, in ionic interlinkages, Asp31 also participates. So, the primary and essential residues of PSKR is Lys158, from phytosulfokine is Thr31 and from SERK1 is simply Asp31. These residues actually play the key role to interact among these three proteins. However, in addition to cation-pi interaction and ionic interaction, these five residues play a central role in the involvement of Van Der Waals energy and electrostatic energy as well as divergent hydrogen bond and hydrophobic interaction, which establish a favorable situation for PSKR, phytosulfokine and SERK1 engagement.

MM/PBSA

Free Binding Energy Contribution

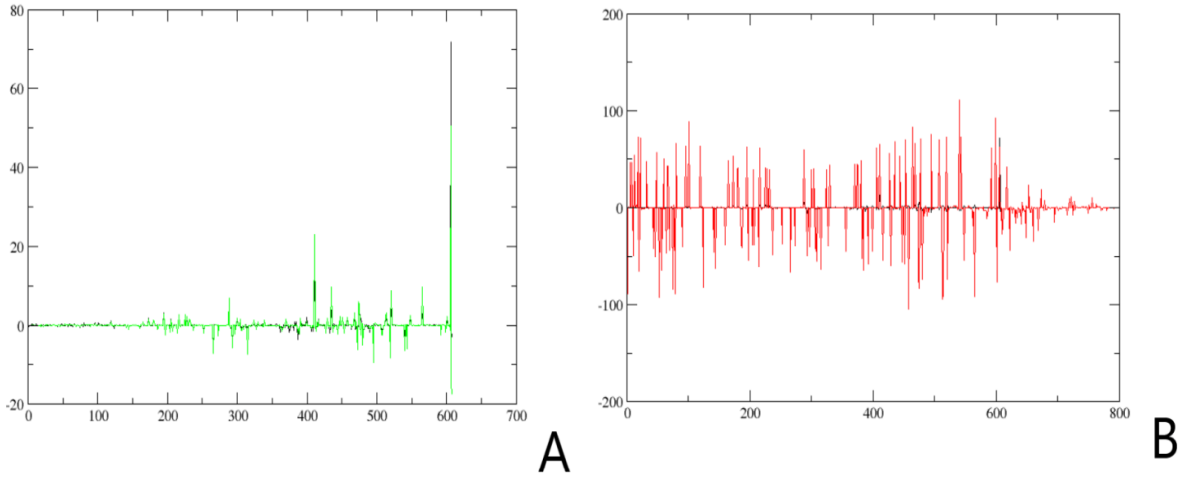

Fig 3.1.1: **(A)** MM/PBSA total energy value from 30ns MD trajectories. PSKR and Phytosulfokine complex (black) presence of Co-receptor SERk1 inside the complex. PSKR and phytosulfokine complex (Green) absence of Co-receptor SERk1. **(B)** MM/PBSA total energy value from 30ns MD trajectories. PSKR and SERk1 complex (Red) presence of PAMP Phytosulfokine inside the complex. PSKR and SERk1 complex (Black) absence of PAMP Phytosulfokine.

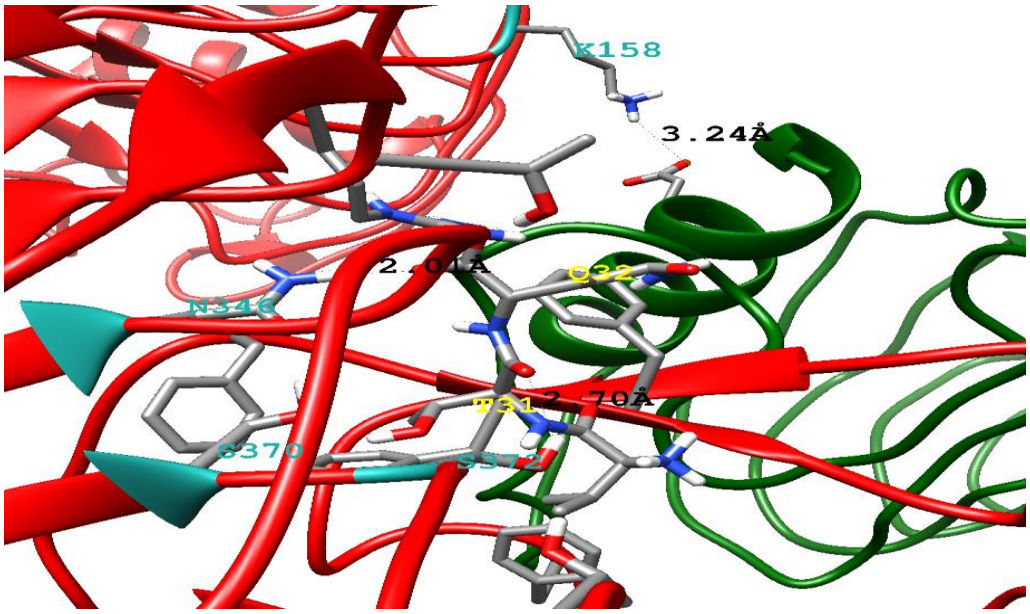

Fig 3.1.2: Cartoon structural view of prominent residues for interacting between PSKR and Phytosulfokine during the presence of Co-receptor SERk1 where the interaction distance is calculated for H-bond.

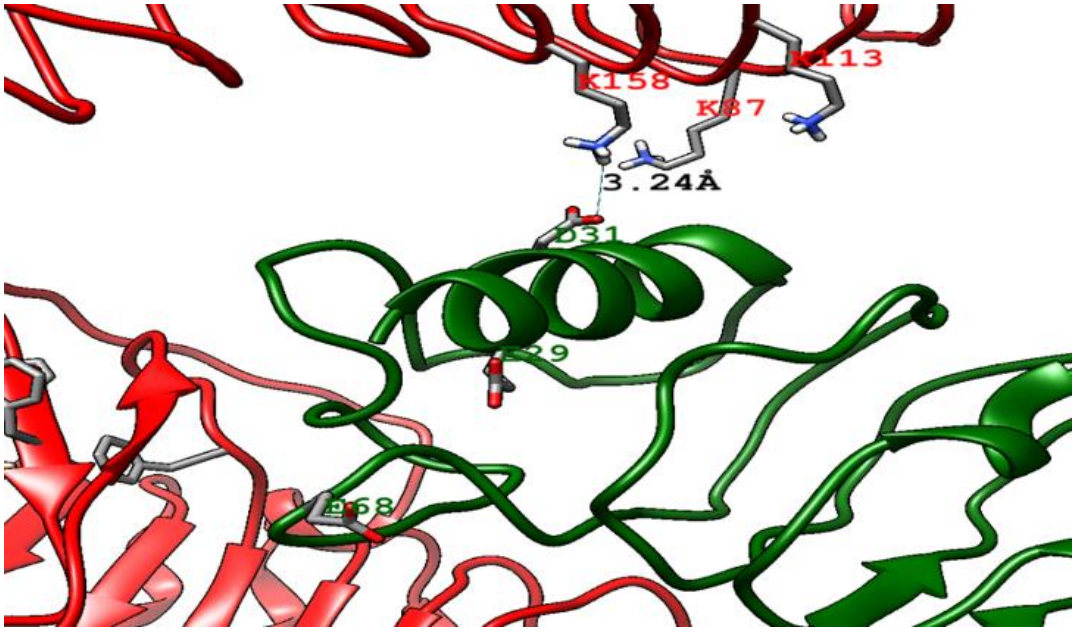

Fig 3.1.3: Cartoon structural view of prominent residues for interacting between PSKR and SERK1 during the presence of PAMP Phytosulfokine where the interaction distance is calculated for H-bond.

Table 3.1.2: Binding free energy contribution of the key binding-site residues calculated from the binding energy decomposition for PSKR (kJmol-1) from PSKR-Phytosulfokine interaction. Marked residues are from three protein complex.

Residues	MM Energy	Polar Energy	Apolar Energy	Total Energy
ARG-109	-0.6663 ± 0.0161	-0.0024 ± 0.0003	0.0000 ± 0.0000	-0.6682 ± 0.0162
ARG-109	-0.2930 ± 0.0264	-0.0047 ± 0.0035	-0.0003 ± 0.0003	-0.2988 ± 0.0264
LYS-158	-0.8442 ± 0.0141	0.0020 ± 0.0002	0.0000 ± 0.0000	-0.8422 ± 0.0141
LYS-158	-0.2754 ± 0.0192	-0.0046 ± 0.0055	0.0003 ± 0.0002	-0.2800 ± 0.0201
ARG-175	-0.6956 ± 0.0104	0.0109 ± 0.0006	0.0000 ± 0.0000	-0.6846 ± 0.0102
ARG-175	-0.6416 ± 0.0104	0.0107 ± 0.0026	-0.0002 ± 0.0003	-0.6305 ± 0.0112
LYS-178	-1.1741 ± 0.0193	0.0350 ± 0.0017	0.0000 ± 0.0000	-1.1380 ± 0.0186
LYS-178	-0.9938 ± 0.0210	0.0271 ± 0.0079	-0.0003 ± 0.0005	-0.9675 ± 0.0231
LYS-194	-0.8610 ± 0.0096	0.0159 ± 0.0008	0.0000 ± 0.0000	-0.8450 ± 0.0088
LYS-194	-0.7996 ± 0.0091	0.0151 ± 0.0054	-0.0007 ± 0.0006	-0.7853 ± 0.0111
LYS-220	-1.0604 ± 0.0119	0.0386 ± 0.0018	0.0000 ± 0.0000	-1.0219 ± 0.0102
LYS-220	-1.0636 ± 0.0108	0.0249 ± 0.0071	0.0008 ± 0.0007	-1.0383 ± 0.0139
ARG-221	-0.8424 ± 0.0102	0.0214 ± 0.0009	0.0000 ± 0.0000	-0.8205 ± 0.0094

ARG-221	-0.8556 ± 0.0106	0.0102 ± 0.0019	-0.0008 ± 0.0004	-0.8459 ± 0.0099
ARG-231	-2.6642 ± 0.0305	0.1020 ± 0.0057	0.0000 ± 0.0000	-2.5624 ± 0.0285
ARG-231	-2.4029 ± 0.0356	0.0302 ± 0.0038	-0.0004 ± 0.0007	-2.3736 ± 0.0330
ARG-238	-1.7772 ± 0.0174	0.0686 ± 0.0031	0.0000 ± 0.0000	-1.7083 ± 0.0146
ARG-238	-1.8504 ± 0.0154	0.0414 ± 0.0047	-0.0006 ± 0.0010	-1.8087 ± 0.0149
ARG-241	-1.4797 ± 0.0144	0.0900 ± 0.0037	0.0000 ± 0.0000	-1.3896 ± 0.0110
ARG-241	-1.5528 ± 0.0141	0.0584 ± 0.0033	-0.0007 ± 0.0005	-1.4954 ± 0.0127
ARG-248	-2.2573 ± 0.0394	0.3003 ± 0.0132	0.0000 ± 0.0000	-1.9558 ± 0.0294
ARG-248	-2.2530 ± 0.0362	0.2235 ± 0.0088	0.0009 ± 0.0004	-2.0292 ± 0.0322
LYS-271	-1.2141 ± 0.0178	0.1041 ± 0.0041	0.0000 ± 0.0000	-1.1092 ± 0.0145
LYS-271	-1.3773 ± 0.0212	0.0859 ± 0.0093	0.0002 ± 0.0004	-1.2921 ± 0.0220
LYS-286	-1.8824 ± 0.0162	0.1090 ± 0.0050	0.0000 ± 0.0000	-1.7731 ± 0.0131
LYS-286	-2.0994 ± 0.0186	0.0796 ± 0.0085	-0.0001 ± 0.0003	-2.0202 ± 0.0203
ARG-300	-13.9191 ± 0.4817	7.0695 ± 0.4613	-0.0500 ± 0.0053	-6.9089 ± 0.1261
ARG-300	-11.6455 ± 0.3475	4.5093 ± 0.3236	-0.0362 ± 0.0058	-7.1805 ± 0.1176
ARG-307	-2.1454 ± 0.0226	0.2354 ± 0.0081	0.0000 ± 0.0000	-1.9105 ± 0.0188
ARG-307	-2.8485 ± 0.0261	0.2495 ± 0.0103	0.0000 ± 0.0005	-2.6004 ± 0.0237
GLY-324	-0.7305 ± 0.0503	0.2733 ± 0.0289	-0.0034 ± 0.0007	-0.4616 ± 0.0298
GLY-324	-0.5295 ± 0.0177	0.2561 ± 0.0105	0.0000 ± 0.0000	-0.2731 ± 0.0102
THR-325	-2.2794 ± 0.1747	1.5829 ± 0.1305	-0.0731 ± 0.0054	-0.7721 ± 0.0772
THR-325	-0.3325 ± 0.0546	0.2812 ± 0.0481	-0.0095 ± 0.0025	-0.0598 ± 0.0214
ARG-327	-6.2649 ± 0.0641	1.0168 ± 0.0387	0.0000 ± 0.0000	-5.2520 ± 0.0487
ARG-327	-6.3859 ± 0.0761	0.5745 ± 0.0217	-0.0002 ± 0.0007	-5.8110 ± 0.0645
ARG-331	-1.2923 ± 0.0370	0.1341 ± 0.0132	0.0000 ± 0.0000	-1.1582 ± 0.0270
ARG-331	-2.5789 ± 0.0269	0.3607 ± 0.0110	0.0000 ± 0.0008	-2.2180 ± 0.0222
ARG-341	-0.8814 ± 0.0205	0.0978 ± 0.0046	0.0000 ± 0.0000	-0.7844 ± 0.0171
ARG-341	-1.3626 ± 0.0220	0.1403 ± 0.0051	-0.0001 ± 0.0006	-1.2239 ± 0.0194
ALA-348	-0.9634 ± 0.0342	0.0481 ± 0.0489	-0.0761 ± 0.0055	-0.9905 ± 0.0557
ALA-348	-0.9042 ± 0.0219	0.5728 ± 0.0173	-0.0087 ± 0.0020	-0.3401 ± 0.0190
SER-372	-2.8567 ± 0.1329	2.7350 ± 0.1177	-0.1910 ± 0.0069	-0.3158 ± 0.0569
SER-372	-3.3884 ± 0.1292	3.1838 ± 0.1306	-0.0878 ± 0.0072	-0.2870 ± 0.0453
VAL-396	-1.3378 ± 0.0506	-0.2802 ± 0.0200	-0.1661 ± 0.0075	-1.7857 ± 0.0537

VAL-396	-0.3567 ± 0.0223	-0.2109 ± 0.0111	-0.0222 ± 0.0028	-0.5877 ± 0.0272
GLU-404	-0.7940 ± 0.0540	0.7547 ± 0.0210	0.0000 ± 0.0000	-0.0392 ± 0.0391
GLU-404	1.7114 ± 0.0429	-0.2867 ± 0.0252	0.0006 ± 0.0004	1.4233 ± 0.0268
ASP-408	-2.4125 ± 0.0159	0.6324 ± 0.0130	0.0000 ± 0.0000	-1.7801 ± 0.0105
ASP-408	-1.0663 ± 0.0243	0.5374 ± 0.0152	-0.0003 ± 0.0005	-0.5287 ± 0.0165
ASP-409	-1.9935 ± 0.0149	0.7389 ± 0.0103	0.0000 ± 0.0000	-1.2551 ± 0.0137
ASP-409	-0.6398 ± 0.0202	0.2520 ± 0.0086	-0.0005 ± 0.0005	-0.3890 ± 0.0156
GLU-415	-1.6326 ± 0.0186	0.4630 ± 0.0071	0.0000 ± 0.0000	-1.1702 ± 0.0139
GLU-415	-0.6724 ± 0.0251	0.2688 ± 0.0105	0.0002 ± 0.0005	-0.4043 ± 0.0202
VAL-421	-2.1187 ± 0.0338	-1.1632 ± 0.0456	-0.4322 ± 0.0075	-3.7148 ± 0.0551
VAL-421	-0.7075 ± 0.0412	-1.1137 ± 0.0177	-0.2059 ± 0.0048	-2.0272 ± 0.0413
ASP-461	-2.9613 ± 0.0217	0.9073 ± 0.0140	0.0000 ± 0.0000	-2.0541 ± 0.0111
ASP-461	-2.7741 ± 0.0237	0.8810 ± 0.0149	0.0001 ± 0.0002	-1.8933 ± 0.0163
GLU-478	-2.7414 ± 0.0218	0.6458 ± 0.0131	0.0000 ± 0.0000	-2.0961 ± 0.0110
GLU-478	-2.7715 ± 0.0219	0.5109 ± 0.0123	-0.0006 ± 0.0006	-2.2620 ± 0.0172
GLU-487	-2.4262 ± 0.0187	0.5090 ± 0.0087	0.0000 ± 0.0000	-1.9173 ± 0.0132
GLU-487	-2.8067 ± 0.0240	0.7948 ± 0.0116	0.0011 ± 0.0010	-2.0095 ± 0.0201
PHE-503	-1.4611 ± 0.0670	0.5453 ± 0.0355	-0.0554 ± 0.0046	-0.9686 ± 0.0385
PHE-503	-0.7214 ± 0.0293	0.1804 ± 0.0136	-0.0071 ± 0.0019	-0.5478 ± 0.0203
PHE-505	-4.7353 ± 0.0914	2.2688 ± 0.0471	-0.3987 ± 0.0078	-2.8663 ± 0.0649
PHE-505	-3.1874 ± 0.0743	1.8739 ± 0.0472	-0.1780 ± 0.0078	-1.4896 ± 0.0433
PHE-506	-13.0952 ± 0.2260	11.4676 ± 0.1911	-1.2826 ± 0.0150	-2.9056 ± 0.1045
PHE-506	-12.3159 ± 0.2594	10.6705 ± 0.2102	-1.1938 ± 0.0154	-2.8403 ± 0.1068
MET-507	-5.8067 ± 0.1205	3.0278 ± 0.0968	-0.2986 ± 0.0067	-3.0772 ± 0.0884
MET-507	-12.7059 ± 0.3406	6.7738 ± 0.2032	-0.2457 ± 0.0084	-6.1670 ± 0.1543
ARG-514	-3.3507 ± 0.0818	0.2455 ± 0.0286	-0.0001 ± 0.0001	-3.1061 ± 0.0634
ARG-514	-6.0804 ± 0.1976	1.1055 ± 0.0920	-0.0147 ± 0.0029	-4.9871 ± 0.1490
ALA-515	-1.7877 ± 0.0575	0.3092 ± 0.0323	-0.2525 ± 0.0076	-1.7322 ± 0.0403
ALA-515	-2.2322 ± 0.0790	1.0372 ± 0.0716	-0.2387 ± 0.0093	-1.4302 ± 0.0411
PHE-524	-2.8222 ± 0.0677	1.4815 ± 0.0520	-0.3558 ± 0.0081	-1.6968 ± 0.0394
PHE-524	-0.8139 ± 0.0423	-0.0325 ± 0.0319	-0.1621 ± 0.0053	-1.0069 ± 0.0293
GLU-529	-16.4005 ± 0.2463	11.8038 ± 0.2809	-0.0001 ± 0.0001	-4.5911 ± 0.0862

GLU-529	-33.8019 ± 0.4043	24.5546 ± 0.5128	-0.1349 ± 0.0067	-9.3820 ± 0.3026
GLU-541	-2.1149 ± 0.0186	0.3782 ± 0.0088	0.0000 ± 0.0000	-1.7381 ± 0.0116
GLU-541	-3.1108 ± 0.0219	0.6258 ± 0.0091	0.0004 ± 0.0003	-2.4847 ± 0.0172
GLU-542	-2.3768 ± 0.0187	0.4888 ± 0.0086	0.0000 ± 0.0000	-1.8890 ± 0.0114
GLU-542	-3.5441 ± 0.0279	1.1399 ± 0.0183	-0.0007 ± 0.0007	-2.4041 ± 0.0161
ASP-553	-8.2444 ± 0.0960	4.8020 ± 0.1046	0.0000 ± 0.0000	-3.4406 ± 0.0478
ASP-553	-14.1079 ± 0.1417	5.9032 ± 0.0957	0.0005 ± 0.0005	-8.2109 ± 0.0943
GLU-574	-3.4951 ± 0.0330	0.8443 ± 0.0150	0.0000 ± 0.0000	-2.6495 ± 0.0259
GLU-574	-8.6749 ± 0.0906	2.3157 ± 0.0459	-0.0004 ± 0.0004	-6.3607 ± 0.0777
ASP-577	-4.8760 ± 0.0473	1.7341 ± 0.0371	0.0000 ± 0.0000	-3.1413 ± 0.0295
ASP-577	-8.1725 ± 0.0796	2.3376 ± 0.0374	-0.0004 ± 0.0003	-5.8325 ± 0.0628
GLU-626	-1.5497 ± 0.0177	0.1311 ± 0.0030	0.0000 ± 0.0000	-1.4191 ± 0.0174
GLU-626	-2.6414 ± 0.0291	0.1853 ± 0.0057	0.0015 ± 0.0009	-2.4554 ± 0.0277
GLU-633	-0.7329 ± 0.0065	0.0151 ± 0.0004	0.0000 ± 0.0000	-0.7176 ± 0.0061
GLU-633	-1.8283 ± 0.0177	0.1101 ± 0.0103	0.0008 ± 0.0008	-1.7175 ± 0.0211

Table 3.1.3: Binding free energy contribution of the key binding-site residues calculated from the binding energy decomposition for PSKR (kJmol-1) PSKR-SERK1 interaction. Marked residues are from three protein complex.

Residue	MM Energy	Polar Energy	Apolar Energy	Total Energy
ARG-30	-83.6018 ± 0.2166	0.1233 ± 0.0668	0.0071 ± 0.0043	-83.4710 ± 0.2238
ARG-30	-88.2926 ± 0.3250	-0.0798 ± 0.070	0.0012 ± 0.0039	-88.3784 ± 0.3421
ARG-40	-49.4973 ± 0.1352	0.0167 ± 0.0276	0.0006 ± 0.0069	-49.4787 ± 0.1397
ARG-40	-49.0353 ± 0.2028	-0.0048 ± 0.027	-0.0051 ± 0.0061	-49.0428 ± 0.200
LYS-49	-65.6478 ± 0.2448	-0.0514 ± 0.062	0.0091 ± 0.0064	-65.6923 ± 0.2411
LYS-49	-65.6941 ± 0.3339	0.2772 ± 0.0653	-0.0074 ± 0.0056	-65.4055 ± 0.3152
ARG-77	-40.1804 ± 0.1160	0.0628 ± 0.0325	0.0054 ± 0.0067	-40.1060 ± 0.1164
ARG-77	-42.4775 ± 0.1466	0.0194 ± 0.0278	0.0031 ± 0.0052	-42.4512 ± 0.1460
ARG-80	-47.6792 ± 0.1725	0.0232 ± 0.0300	-0.0043 ± 0.0059	-47.6614 ± 0.1656
ARG-80	-50.7469 ± 0.1798	0.0266 ± 0.0244	-0.0018 ± 0.0041	-50.7206 ± 0.1865
LYS-86	-63.1318 ± 0.2679	0.0405 ± 0.0652	-0.0053 ± 0.0068	-63.0885 ± 0.2747
LYS-86	-69.0060 ± 0.3841	0.2663 ± 0.0635	-0.0024 ± 0.0036	-68.7733 ± 0.3773

LYS-87	-86.2544 ± 0.5341	0.3126 ± 0.1805	-0.0136 ± 0.0064	-85.9527 ± 0.4944
LYS-87	-105.4179 ± 1.110	13.3308 ± 1.14	-0.2428 ± 0.0211	-92.2834 ± 0.51
LYS-91	-71.2261 ± 0.4216	-0.0025 ± 0.079	0.0003 ± 0.0076	-71.2130 ± 0.4215
LYS-91	-64.6023 ± 0.3642	0.1126 ± 0.0636	0.0017 ± 0.0049	-64.4896 ± 0.3612
LYS-98	-48.2101 ± 0.1467	0.0392 ± 0.0722	-0.0058 ± 0.0059	-48.1832 ± 0.1664
LYS-98	-46.5746 ± 0.1773	0.0817 ± 0.0573	-0.0012 ± 0.0039	-46.4935 ± 0.1935
ARG-103	-41.9316 ± 0.1129	0.0470 ± 0.0285	-0.0032 ± 0.0058	-41.8929 ± 0.1218
ARG-103	-43.6130 ± 0.1420	0.0070 ± 0.0247	-0.0022 ± 0.0038	-43.6027 ± 0.1465
ARG-109	-73.4827 ± 0.4552	-0.1043 ± 0.043	-0.0005 ± 0.0050	-73.6124 ± 0.459
ARG-109	-83.6302 ± 0.5141	-0.1239 ± 0.086	-0.0300 ± 0.0065	-83.7876 ± 0.479
LYS-113	-94.5144 ± 0.7078	0.8395 ± 0.2731	-0.0093 ± 0.0052	-93.6761 ± 0.6071
LYS-113	-96.4352 ± 1.0603	8.1238 ± 0.7876	-0.0693 ± 0.0080	-88.2790 ± 0.5884
LYS-124	-40.1631 ± 0.1140	0.0997 ± 0.0730	-0.0113 ± 0.0064	-40.0726 ± 0.1320
LYS-124	-40.4573 ± 0.1382	-0.0734 ± 0.061	0.0070 ± 0.0037	-40.5270 ± 0.1470
LYS-158	-87.6139 ± 0.7266	1.1010 ± 0.2637	-0.0049 ± 0.0055	-86.5232 ± 0.6262
LYS-158	-87.0473 ± 0.9329	5.3241 ± 0.5955	-0.0510 ± 0.0074	-81.7883 ± 0.6353
ARG-175	-44.6824 ± 0.1487	-0.0499 ± 0.032	0.0044 ± 0.0059	-44.7246 ± 0.1511
ARG-175	-45.4151 ± 0.1259	-0.0405 ± 0.025	-0.0078 ± 0.0035	-45.4644 ± 0.131
LYS-178	-58.8704 ± 0.2356	-0.0996 ± 0.062	-0.0050 ± 0.0073	-58.9764 ± 0.242
LYS-178	-62.5064 ± 0.2136	-0.2141 ± 0.059	0.0023 ± 0.0065	-62.7228 ± 0.2243
LYS-194	-38.4294 ± 0.0971	0.0344 ± 0.0644	0.0076 ± 0.0049	-38.3889 ± 0.1192
LYS-194	-38.3110 ± 0.0893	0.0396 ± 0.0545	-0.0044 ± 0.0035	-38.2743 ± 0.1070
LYS-220	-36.9844 ± 0.0648	0.1041 ± 0.0593	0.0006 ± 0.0036	-36.8775 ± 0.0864
LYS-220	-37.8717 ± 0.0634	-0.0392 ± 0.056	0.0044 ± 0.0038	-37.9054 ± 0.0851
ARG-221	-39.9966 ± 0.0890	0.0362 ± 0.0339	-0.0135 ± 0.0054	-39.9743 ± 0.0963
ARG-221	-40.6905 ± 0.1114	-0.0166 ± 0.027	-0.0021 ± 0.0034	-40.7170 ± 0.117
ARG-231	-54.7334 ± 0.2037	0.0865 ± 0.0311	-0.0049 ± 0.0046	-54.6626 ± 0.2236
ARG-231	-53.4100 ± 0.2265	-0.7158 ± 0.117	-0.0085 ± 0.0040	-54.1423 ± 0.238
ARG-238	-37.0352 ± 0.0622	0.0328 ± 0.0329	0.0045 ± 0.0065	-36.9979 ± 0.0699
ARG-238	-38.6014 ± 0.0667	0.0257 ± 0.0321	0.0024 ± 0.0055	-38.5769 ± 0.0727
ARG-241	-36.6114 ± 0.0546	0.0154 ± 0.0327	-0.0052 ± 0.0070	-36.6006 ± 0.0635
ARG-241	-38.0068 ± 0.0583	0.0035 ± 0.0265	-0.0062 ± 0.0060	-38.0093 ± 0.0639

LYS-271	-46.1451 ± 0.0988	0.0758 ± 0.0666	0.0047 ± 0.0042	-46.0721 ± 0.1163
LYS-271	-48.1065 ± 0.1098	-0.0028 ± 0.056	-0.0029 ± 0.0031	-48.1062 ± 0.122
LYS-286	-36.2973 ± 0.0484	0.0874 ± 0.0658	0.0024 ± 0.0043	-36.2044 ± 0.0765
LYS-286	-37.2624 ± 0.0485	-0.0374 ± 0.060	-0.0010 ± 0.0031	-37.2965 ± 0.075
ARG-300	-63.5847 ± 0.1191	0.5667 ± 0.0304	0.0069 ± 0.0053	-63.0142 ± 0.1143
ARG-300	-70.4054 ± 0.1993	3.8880 ± 0.0674	-0.0030 ± 0.0044	-66.5208 ± 0.1563
ARG-307	-37.7952 ± 0.0503	0.0756 ± 0.0367	0.0129 ± 0.0063	-37.7068 ± 0.0628
ARG-307	-38.9705 ± 0.0738	0.0647 ± 0.0312	0.0003 ± 0.0045	-38.9064 ± 0.0770
ARG-327	-46.4175 ± 0.0993	0.0909 ± 0.0325	0.0052 ± 0.0046	-46.3231 ± 0.1043
ARG-327	-49.8394 ± 0.1553	0.1248 ± 0.0292	0.0018 ± 0.0037	-49.7115 ± 0.1603
ARG-331	-38.3687 ± 0.0502	0.1444 ± 0.0378	0.0052 ± 0.0069	-38.2214 ± 0.0650
ARG-331	-40.0768 ± 0.0501	0.1975 ± 0.0320	-0.0085 ± 0.0056	-39.8866 ± 0.0565
LYS-340	-39.9020 ± 0.0463	0.0720 ± 0.0662	0.0041 ± 0.0055	-39.8280 ± 0.0779
LYS-340	-40.9482 ± 0.0472	0.0925 ± 0.0593	-0.0008 ± 0.0044	-40.8548 ± 0.0712
ARG-341	-44.1830 ± 0.0832	0.0336 ± 0.0348	0.0037 ± 0.0056	-44.1471 ± 0.0831
ARG-341	-45.0072 ± 0.0855	0.1261 ± 0.0280	0.0008 ± 0.0035	-44.8814 ± 0.0926
LYS-343	-54.3521 ± 0.1289	0.1412 ± 0.0614	-0.0068 ± 0.0053	-54.2192 ± 0.1472
LYS-343	-55.3147 ± 0.1279	0.3906 ± 0.0589	-0.0012 ± 0.0048	-54.9121 ± 0.1359
ARG-349	-60.6347 ± 0.1619	0.3498 ± 0.0349	-0.0002 ± 0.0033	-60.2887 ± 0.1576
ARG-349	-65.5745 ± 0.2700	2.2603 ± 0.0730	-0.0056 ± 0.0032	-63.3189 ± 0.2075
LYS-361	-38.6189 ± 0.0451	0.0924 ± 0.0734	-0.0044 ± 0.0072	-38.5262 ± 0.0827
LYS-361	-39.7034 ± 0.0364	0.1466 ± 0.0654	-0.0065 ± 0.0062	-39.5602 ± 0.0737
LYS-390	-42.9838 ± 0.0515	0.2087 ± 0.0661	-0.0066 ± 0.0062	-42.7779 ± 0.0801
LYS-390	-44.8081 ± 0.0616	0.3896 ± 0.0577	-0.0004 ± 0.0044	-44.4195 ± 0.0807
LYS-416	-49.6144 ± 0.0912	0.2310 ± 0.0686	0.0000 ± 0.0067	-49.3843 ± 0.1053
LYS-416	-52.3038 ± 0.1133	0.4387 ± 0.0572	-0.0063 ± 0.0040	-51.8680 ± 0.1213
LYS-418	-62.4265 ± 0.1500	0.9152 ± 0.0600	0.0079 ± 0.0066	-61.5096 ± 0.1438
LYS-418	-67.9956 ± 0.2109	3.7504 ± 0.0714	0.0020 ± 0.0035	-64.2379 ± 0.1761
ARG-426	-51.7754 ± 0.1676	0.2563 ± 0.0331	0.0061 ± 0.0061	-51.5120 ± 0.1608
ARG-426	-58.5863 ± 0.1247	0.7312 ± 0.0255	0.0062 ± 0.0041	-57.8518 ± 0.1218
ARG-433	-46.0392 ± 0.0842	0.1676 ± 0.0321	-0.0014 ± 0.0052	-45.8742 ± 0.0882
ARG-433	-45.2495 ± 0.0753	0.2179 ± 0.0294	-0.0060 ± 0.0054	-45.0370 ± 0.0790

ARG-450	-55.7534 ± 0.1706	0.5000 ± 0.0317	-0.0023 ± 0.0056	-55.2583 ± 0.1695
ARG-450	-55.2139 ± 0.1208	0.8257 ± 0.0277	0.0030 ± 0.0040	-54.3920 ± 0.1183
LYS-463	-58.1443 ± 0.1288	0.4013 ± 0.0683	-0.0123 ± 0.0072	-57.7528 ± 0.1435
LYS-463	-60.9076 ± 0.1344	0.7287 ± 0.0585	-0.0001 ± 0.0046	-60.1728 ± 0.1406
LYS-481	-53.8739 ± 0.0888	0.5667 ± 0.0612	0.0036 ± 0.0048	-53.3056 ± 0.1036
LYS-481	-56.7547 ± 0.1592	0.7213 ± 0.0577	0.0059 ± 0.0049	-56.0294 ± 0.1550
LYS-485	-56.0942 ± 0.1209	0.4190 ± 0.0703	-0.0032 ± 0.0059	-55.6789 ± 0.1337
LYS-485	-58.6814 ± 0.1015	0.8320 ± 0.0576	-0.0056 ± 0.0057	-57.8582 ± 0.1121
ARG-492	-106.7721 ± 0.628	2.7035 ± 0.240	-0.0688 ± 0.0097	-104.1249 ± 0.49
ARG-492	-152.2550 ± 0.880	49.3453 ± 0.85	-1.5760 ± 0.0219	-104.4975 ± 0.3
LYS-508	-77.6407 ± 0.3394	5.6747 ± 0.1957	-0.0002 ± 0.0067	-71.9700 ± 0.2133
LYS-508	-75.9197 ± 0.2426	4.2128 ± 0.1056	-0.0022 ± 0.0042	-71.6992 ± 0.1818
ARG-509	-96.6419 ± 0.4316	5.0071 ± 0.1656	-0.0630 ± 0.0088	-91.7212 ± 0.3630
ARG-509	-134.8584 ± 1.471	52.9770 ± 1.43	-0.9558 ± 0.0337	-82.8731 ± 0.2501
ARG-514	-127.5172 ± 1.067	52.4303 ± 1.1692	-1.7018 ± 0.0264	-76.7606 ± 0.4150
ARG-514	-83.9748 ± 0.8528	10.1506 ± 0.773	-0.3283 ± 0.0220	-74.1496 ± 0.3168
LYS-547	-83.4504 ± 0.2302	1.1594 ± 0.0633	0.0009 ± 0.0057	-82.2943 ± 0.2321
LYS-547	-97.2830 ± 0.3672	3.3928 ± 0.1074	-0.0015 ± 0.0061	-93.8923 ± 0.3332
LYS-548	-108.2394 ± 0.369	6.6631 ± 0.312	-0.0704 ± 0.0099	-101.6404 ± 0.3141
LYS-548	-111.0137 ± 0.655	21.6623 ± 0.91	-0.2259 ± 0.0125	-89.5402 ± 0.5148
LYS-555	-77.9235 ± 0.2641	1.3776 ± 0.0664	-0.0028 ± 0.0048	-76.5563 ± 0.2740
LYS-555	-77.4596 ± 0.1385	3.3579 ± 0.0532	0.0014 ± 0.0030	-74.1018 ± 0.1321
ARG-582	-54.2076 ± 0.1741	0.4763 ± 0.0342	0.0033 ± 0.0062	-53.7343 ± 0.1652
ARG-582	-54.2032 ± 0.0876	0.5130 ± 0.0315	-0.0020 ± 0.0067	-53.6918 ± 0.0867
LYS-599	-151.8072 ± 1.084	79.9082 ± 1.5700	-0.9213 ± 0.016	-72.8004 ± 0.6562
LYS-599	-108.4803 ± 0.554	17.0134 ± 0.38	-0.0735 ± 0.0073	-91.5300 ± 0.3941
ARG-635	-72.0394 ± 0.6142	3.2165 ± 0.4392	-0.6014 ± 0.0208	-69.4197 ± 0.3022
ARG-635	-91.6653 ± 0.5998	16.3478 ± 0.612	-0.8338 ± 0.0253	-76.1374 ± 0.3218

Table 3.1.4: Binding free energy contribution of the key binding-site residues calculated from the binding energy decomposition for Phytosulfokine (kJmol-1) PSKR-Phytosulfokine interaction. Marked residues are from three protein complex.

Residue	MM Energy	Polar Energy	Apolar Energy	Total Energy
THR-31	-21.2975 ± 0.3434	20.0159 ± 0.2818	-2.5223 ± 0.0167	-3.8066 ± 0.1797
THR-31	-40.5678 ± 0.4988	28.1400 ± 0.3588	-2.4759 ± 0.0195	-14.8964 ± 0.2438
GLN-32	-117.8896 ± 0.8207	119.2362 ± 1.3447	-3.5545 ± 0.0240	-2.1566 ± 0.7372
GLN-32	-115.1895 ± 1.1424	100.9623 ± 1.6353	-3.2948 ± 0.0311	-17.4842 ± 0.8586

Table 3.1.5: Binding free energy contribution of the key binding-site residues calculated from the binding energy decomposition for SERK1 (kJmol-1) PSKR-SERK1 interaction. Marked residues are from three protein complex.

Residue	MM Energy	Polar Energy	Apolar Energy	Total Energy
GLU-29	-48.9972 ± 0.6057	14.1781 ± 0.674	-0.0297 ± 0.0092	-34.8427 ± 0.329
GLU-29	-29.2876 ± 0.2462	2.1146 ± 0.1277	0.0105 ± 0.0084	-27.1578 ± 0.2174
ASP-31	-28.7104 ± 0.3649	1.8001 ± 0.2024	-0.0242 ± 0.0074	-26.9203 ± 0.3336
ASP-31	-26.2942 ± 0.4374	3.4931 ± 0.4339	-0.0327 ± 0.0090	-22.8350 ± 0.4040
ASP-42	-37.5365 ± 0.2966	-1.1552 ± 0.121	-0.0117 ± 0.0069	-38.6937 ± 0.249
ASP-42	-50.0711 ± 0.3829	6.0372 ± 0.2458	0.0123 ± 0.0072	-44.0446 ± 0.2704
ASP-51	-36.0653 ± 0.4282	-2.2587 ± 0.231	-0.0219 ± 0.0057	-38.3449 ± 0.388
ASP-51	-63.8608 ± 0.9271	49.0028 ± 1.488	-1.1379 ± 0.0202	-16.0425 ± 0.718
GLU-68	-69.1150 ± 0.7803	32.0690 ± 0.784	-0.8951 ± 0.0221	-37.9615 ± 0.402
GLU-68	-34.6577 ± 0.5100	3.7676 ± 0.3441	-0.0578 ± 0.0084	-30.9545 ± 0.3275
GLU-80	-29.4906 ± 0.2729	-0.2506 ± 0.104	-0.0027 ± 0.0090	-29.7336 ± 0.263
GLU-80	-36.0719 ± 0.3547	1.8676 ± 0.1372	-0.0141 ± 0.0093	-34.2148 ± 0.3180
GLU-88	-22.7662 ± 0.3112	1.2729 ± 0.1890	-0.0067 ± 0.0073	-21.5094 ± 0.2777
GLU-88	-28.0097 ± 0.4432	4.7467 ± 0.4621	-0.0590 ± 0.0111	-23.3370 ± 0.3227
ASP-115	-16.2286 ± 0.1529	0.8170 ± 0.0846	-0.0003 ± 0.0076	-15.4055 ± 0.1694
ASP-115	-15.6878 ± 0.1529	0.4611 ± 0.0911	0.0078 ± 0.0064	-15.2100 ± 0.1795
PHE-145	-12.3189 ± 0.0907	4.3128 ± 0.0401	-1.3533 ± 0.0152	-9.3633 ± 0.0867
PHE-145	-9.0429 ± 0.2119	3.0810 ± 0.0852	-1.1382 ± 0.0300	-7.0987 ± 0.1683

3.2 Root Mean Square Fluctuation (RMSF)

The RMSFs of the PSKR, phytosulfokine and SERK1 residues were determined from the MD trajectories in this simulated scheme. To measure the RMSF values, 30ns were utilized. The findings demonstrate that most of the residues usually ranges from less than 0.40 nm for PSKR to 0.11 nm for phytosulfokine to 0.30 nm for SERK1(Fig 3.2.1). However, several other residues for PSKR reach 0.45 nm, 0.13 nm for phytosulfokine and 0.35 nm for SERK1. Few residues suggest the most favorable state for interaction between proteins from the MM/PBSA evaluation. Arg300, Arg327, Met507, Arg514, Glu529, Asp553, Glu574 have additional favorable status for PSKR either way (when SERK1 is present in the complex and absent in the complex). In addition, it is acquired from the graphical interface perspective of RMSF that such residues have less fluctuation in divergence to other PSKR residues. When an encounter between PSKR and SERK1 takes place then the most prominent residue of PSKR Arg300 displays the lowest fluctuation (0.15 nm) in RMSF when phytosulfokine is present inside the complex and shows the second-lowest fluctuation in the absence of phytosulfokine (0.13 nm). Asp51 (0.44 nm) and Ser57 (0.43 nm) are the most fluctuated residues of PSKR in the phytosulfokine company, but also when there is no phytosulfokine in the Ser57 complex, this specification also has the highest fluctuation. In the case of phytosulfokine, the minimal fluctuation in RMSF is shown by Thr31, as another relevant residue is shown in the MM/PBSA estimation. phytosulfokine remains at 0.08 nm when SERK1 is present in the complex during contact with PSKR Thr31 and it goes down to 0.07 nm when SERK1 is omitted from the complex. The additional phytosulfokine residue is Gln32, which is very little fluctuating residue in the complex where SERK1 subsists, but the same fluctuating residue persists after withdrawing SERK1 from the Gln32 complex (0.11nm). On the counter, in the context of PSKR and SERK1, the PSKR interlinkages Arg30, Lys87, Arg109, Lys113, Lys158, Arg492, Lys547, Lys548, Lys599 provide the minimum rate of fluctuation for both the circumstances wherein phytosulfokine is present in and withdrawn from the complex. These residues of PSKR also provide extra energy for interacting with SERK1 from the estimation of MM/PBSA. PSKR Lys158, which provides the lowest RMSF value (0.18nm) when phytosulfokine is present in the complex and the fluctuation rate of Lys158 is 0.23 nm during the absence of phytosulfokine in the complex, suggesting that it remains the most prevalent residue as indicated in the MM/PBSA analysis. Furthermore, it has been already demonstrated that Asp51 and Ser57 are

the key fluctuating residues of PSKR in this interaction. Glu29, Asp31, Asp42 for SERK1. The most significant residues are listed as Asp51, Glu68, Glu80 by MM/PBSA measurement. These residues also have fewer variations in the deviation of other SERK1 residues in the RMSF graphical outline. Asp31 has the most negligible fluctuation value (0.16 nm) among these residues, when phytosulfokine is present. On the other hand, without phytosulfokine, it fluctuates somewhat down to 0.14 nm. Though several other lowest fluctuated residues are observed from the RMSF assessment and some highly fluctuated residues are also identified, the indicated residues are primarily in charge in terms of the interaction between PSKR, phytosulfokine and SERK1. In addition, the involvement of Co-Receptor SERK1 in the complex is mandatory for the ongoing interaction between PSKR and phytosulfokine. In addition to the fact that the fluctuation rate of the residues of PSKR and phytosulfokine declines after elimination of SERK1, that increases the possibilities of interaction among them.

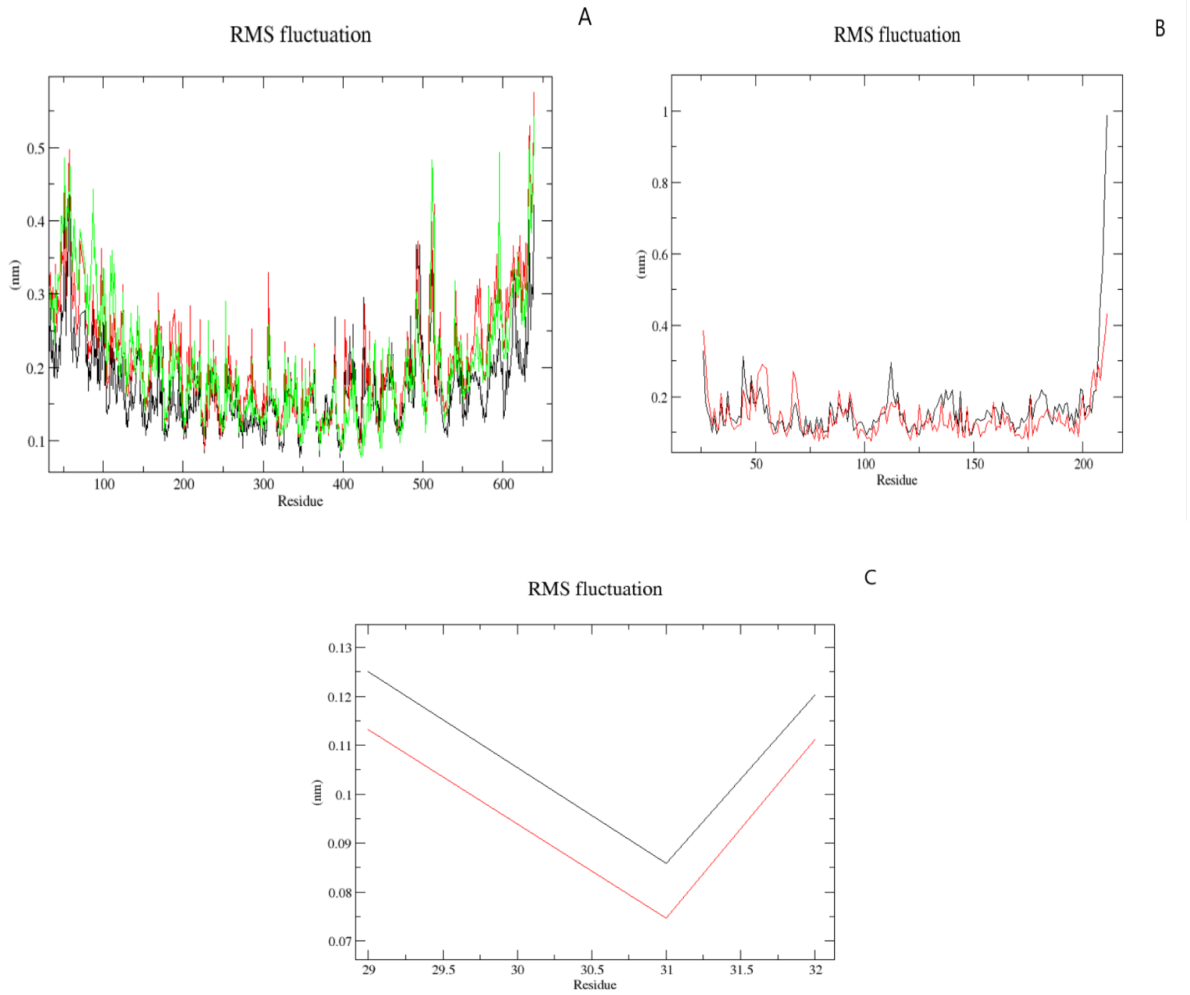

Fig 3.2.1: (A) RMSF value of PSKR from 30ns MD trajectories. PSKR, Phytosulfokine complex (Black) presence of SERk1 in the complex, PSKR and Phytosulfokine complex (Red)

absence of SERk1, PSKR and SERk1 complex (Green) absence of Phytosulfokine**(B)** RMSF value of SERk1 from 30ns MD trajectories. PSKR, SERk1 complex (Black) in the presence of Phytosulfokine, PSKR and SERk1 complex (Red) absence of Phytosulfokine **(C)** RMSF value of Phytosulfokine from 30ns MD trajectories. PSKR, Phytosulfokine complex (black) presence of SERk1, PSKR and Phytosulfokine complex (red) absence of SERk1.

3.3 H-Bond

Quantity of hydrogen bonds was estimated over the simulation duration of 30 ns for protein-protein norms. The protein-protein hydrogen bonds illustrate the lifting graph of the entire curve in the simulation. For a greater grasp of the development of hydrogen bond inside two protein index files, it was used to quantify the structure of the total hydrogen bond at a divergent duration of time. It is evident from Fig 3.3.1(A) that a maximum of 9 hydrogen bonds among PSKR and phytosulfokine are located at 19600ps while SERK1 is included and a maximum of 11 hydrogen bonds are formed at 25300ps and 25850ps in the nonexistence of SERK1. Protein Interaction Calculation (PIC) (Table 3.3.1-3.3.21) data also revealed that very few feasible hydrogen bond interactions take place between PSKR and phytosulfokine, with a relatively significant number of sustainable hydrogen bond interactions among PSKR and SERK1. Asp31 of SERK1 adds atoms to PSKR's Lys158 to form ionic interaction in considerable detail. Further, in the involvement of SERK1 and main chain-side chain interaction with Phe506 in the absence of PSKR SERK1, phytosulfokine Thr31 also creates the side chain side chain with Ser370. The number of all possible interactions is illustrated on the basis of PIC outcomes (Table 3.3.22). Where 7 hydrogen bonds are located at the very initial level or even before simulation, 6 hydrophobic interactions have taken place among PSKR and phytosulfokine when SERK1 is also associated with them. Although the number of hydrogen bonds is reduced after the 30ns simulation stage between PSKR and phytosulfokine in this condition, hydrophobic interactions are also reduced and the sole ionic interaction is produced. In addition, the complex hydrogen bonds of PSKR and phytosulfokine are somewhat strengthened when SERK1 is absent. On the reverse, the percentage of PSKR and SERK1 hydrogen bonds is 14 prior to the simulation. In the exclusion of phytosulfokine, the PSKR and SERK1 hydrogen bond numbers remain the same. In all cases, reduction of hydrophobic and ionic interactions is prolific. In many other cases, while 14 hydrogen bonds were identified among PSKR and SERK1 before the simulation, hydrogen bonds were increased significantly to 24

before the simulation. This tends to happen when phytosulfokine is present in the complex as well as the hydrogen bond numbers of PSKR and SERK1 are decreased to 22 and during absence of phytosulfokine. Hardly any minimal additional fundamental interactions among PSKR and phytosulfokine have been found.

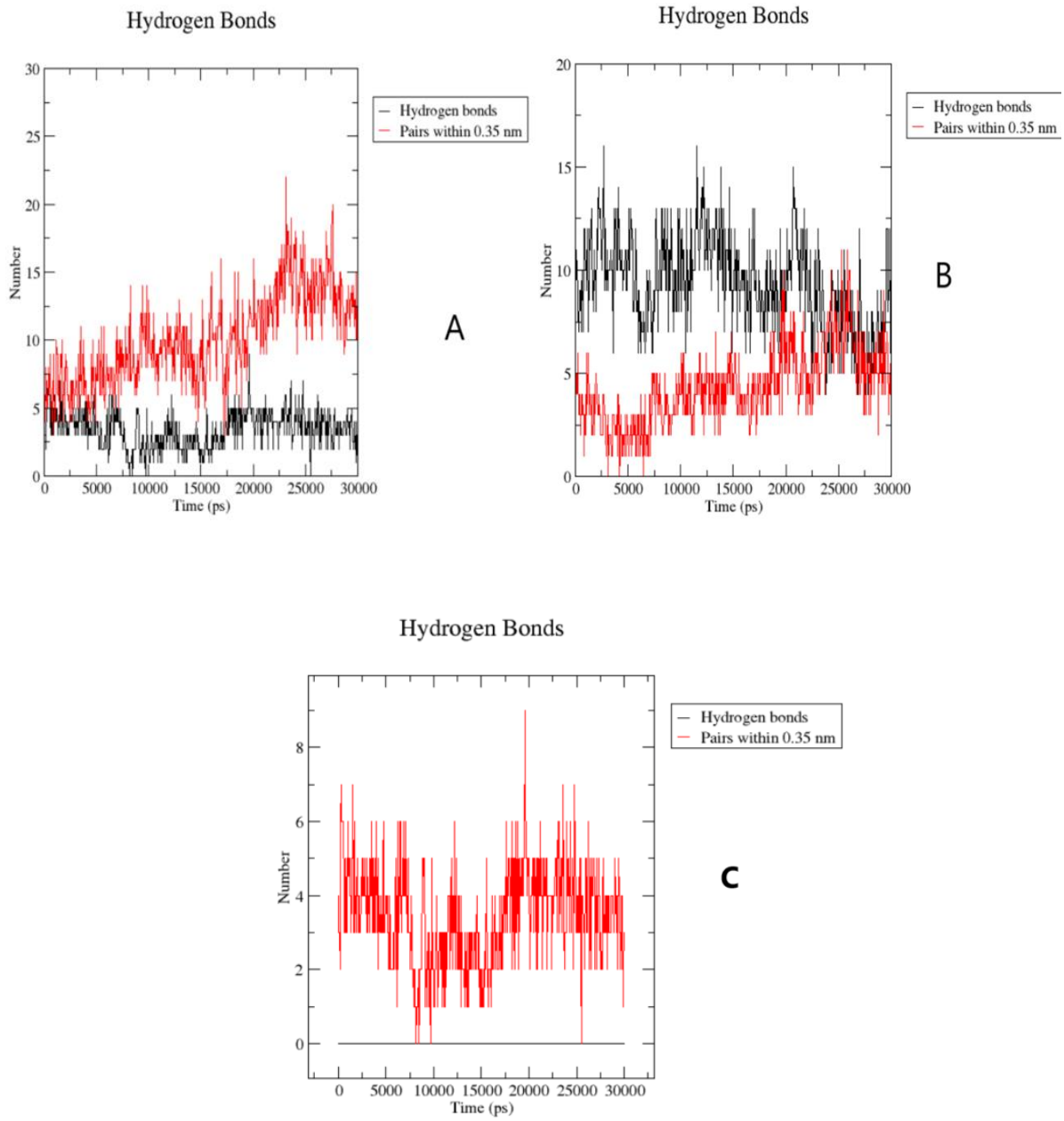

Fig 3.3.1: (A) H-bond value of PSKR and Phytosulfokine from 30ns MD trajectories. PSKR, Phytosulfokine complex (Black) presence of SERk1 in the complex, PSKR and Phytosulfokine complex (Red) absence of SERk1. **(B)** H-bond value of PSKR and SERk1 from 30ns MD trajectories. PSKR, SERk1 complex (Black) in the presence of Phytosulfokine, PSKR and SERk1 complex (Red) absence of Phytosulfokine. **(C)** H-bond value of Phytosulfokine and

SERk1 from 30ns MD trajectories. Phytosulfokine and SERk1 complex, here it is observed that without phytosulfokine SERK1 and PSKR has no interaction.

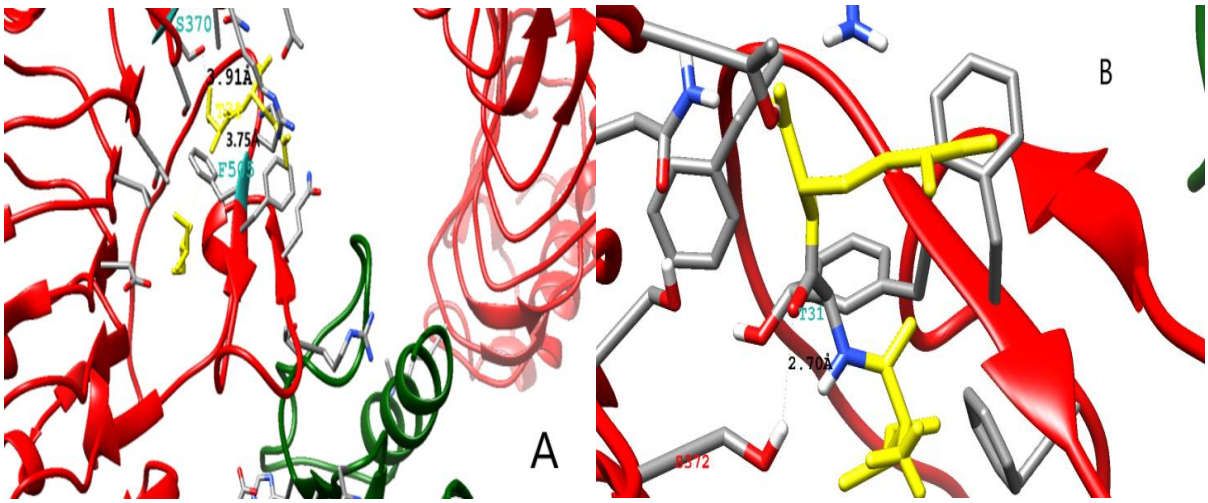

Fig 3.3.2: (A) H-bond of **THR31** from Phytosulfokine before simulation in cartoon structure. **(B)** H-bond of **THR31** from Phytosulfokine After simulation in cartoon structure.

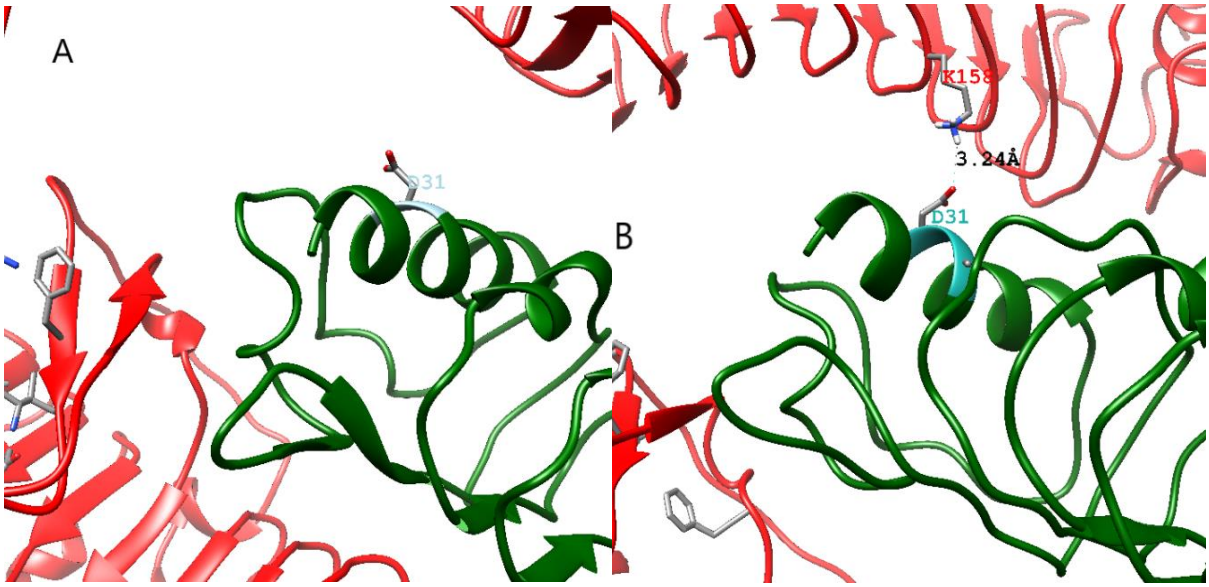

Fig 3.3.3: (A) H-bond of **ASP31** from SERk1 before simulation in cartoon structure. **(B)** H-bond of **ASP31** from SERk1 After simulation in cartoon structure.

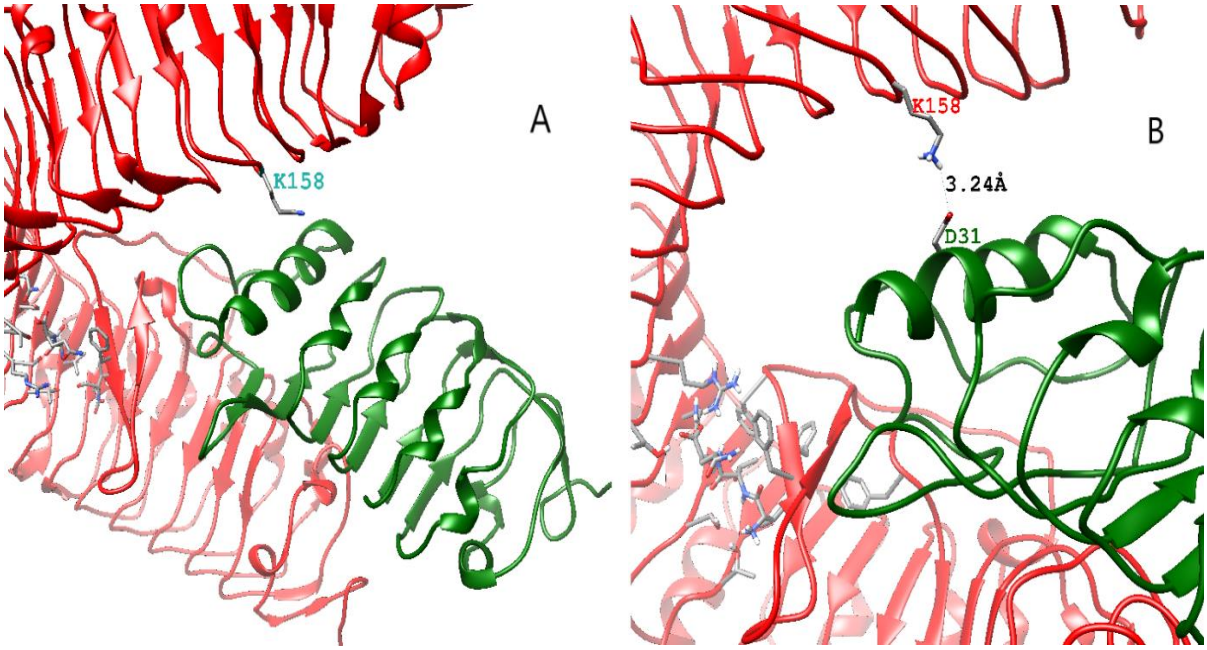

Fig 3.3.4: (A) H-bond of **LYS158** from PSKR before simulation in cartoon structure. **(B)** H-bond of **LYS158** from PSKR After simulation in cartoon structure.

Table 3.3.1: Protein-Protein Hydrophobic Interactions of PSKR-Phytosulfokine-SERk1 complex before and after simulation.

Before Simulation					
Position	**Residue**	**Chain**	**Position**	**Residue**	**Chain**
111	PHE	A	38	VAL	C
421	VAL	A	29	ILE	P
443	LEU	A	29	ILE	P
467	TYR	A	29	ILE	P
505	PHE	A	29	ILE	P
507	MET	A	29	ILE	P
524	PHE	A	29	ILE	P
525	PRO	A	61	PHE	C
526	PRO	A	61	PHE	C
596	PHE	A	46	VAL	C
596	PHE	A	79	ALA	C

After Simulation					
Position	**Residue**	**Chain**	**Position**	**Residue**	**Chain**
111	PHE	A	38	VAL	C
396	VAL	A	29	ILE	P
421	VAL	A	29	ILE	P
505	PHE	A	29	ILE	P
507	MET	A	29	ILE	P
524	PHE	A	29	ILE	P
525	PRO	A	61	PHE	C
596	PHE	A	76	LEU	C
596	PHE	A	79	ALA	C
621	PRO	A	97	TYR	C

Table 3.3.2: Protein-Protein Main Chain-Main Chain Hydrogen Bonds of PSKR-Phytosulfokine-SERk1 complex before and after simulation.

Before Simulation								
DONOR				**ACCEPTOR**				
POS	**CHAIN**	**RES**	**ATOM**	**POS**	**CHAIN**	**RES**	**ATOM**	**Dd-a**
325	A	THR	N	32	P	GLN	O	3.46
After Simulation								
DONOR				**ACCEPTOR**				
POS	**CHAIN**	**RES**	**ATOM**	**POS**	**CHAIN**	**RES**	**ATOM**	**Dd-a**
506	A	PHE	N	29	P	ILE	O	2.76

Table 3.3.3: Protein-Protein Main Chain-Side Chain Hydrogen Bonds of PSKR-Phytosulfokine-SERk1 complex before and after simulation.

Before Simulation								
DONOR				**ACCEPTOR**				
POS	**CHAIN**	**RES**	**ATOM**	**POS**	**CHAIN**	**RES**	**ATOM**	**Dd-a**
87	A	LYS	NZ	38	C	VAL	O	3.28

325	A	THR	OG1	32	P	GLN	O	2.61
346	A	ASN	ND2	32	P	GLN	OXT	2.9
346	A	ASN	ND2	32	P	GLN	OXT	2.9
398	A	THR	OG1	29	P	ILE	O	2.73
595	A	SER	OG	77	C	GLY	O	2.97
62	C	HIS	N	574	A	GLU	OE2	2.83
73	C	ARG	NH1	619	A	THR	O	3.01
73	C	ARG	NH1	619	A	THR	O	3.01
29	P	ILE	N	445	A	ASP	OD2	2.95
31	P	THR	N	372	A	SER	OG	3.2
After Simulation								
DONOR				**ACCEPTOR**				
POS	**CHAIN**	**RES**	**ATOM**	**POS**	**CHAIN**	**RES**	**ATOM**	**Dd-a**
514	A	ARG	NE	67	C	ASN	O	3.43
595	A	SER	OG	77	C	GLY	O	2.64
59	C	THR	OG1	517	A	GLN	O	2.75
62	C	HIS	N	574	A	GLU	OE1	2.93
73	C	ARG	NH2	597	A	LEU	O	3.11
73	C	ARG	NH2	597	A	LEU	O	3.11
73	C	ARG	NE	598	A	SER	O	3.41
73	C	ARG	NH1	598	A	SER	O	3.42
73	C	ARG	NH1	598	A	SER	O	3.42
75	C	ASP	OD1	597	A	LEU	O	3.26
75	C	ASP	OD1	597	A	LEU	O	3.26

Table 3.3.4: Protein-Protein Side Chain-Side Chain Hydrogen Bonds of PSKR-Phytosulfokine-SERk1 complex before and after simulation.

Before Simulation								
DONOR				**ACCEPTOR**				
POS	**CHAIN**	**RES**	**ATOM**	**POS**	**CHAIN**	**RES**	**ATOM**	**Dd-a**
349	A	ARG	NH1	32	P	GLN	OE1	3.16
349	A	ARG	NH1	32	P	GLN	OE1	3.16

616	A	GLN	NE2	75	C	ASP	OD1	3.07
616	A	GLN	NE2	75	C	ASP	OD1	3.07
616	A	GLN	OE1	101	C	TYR	OH	2.43
616	A	GLN	OE1	101	C	TYR	OH	2.43
75	C	ASP	OD1	616	A	GLN	NE2	3.07
75	C	ASP	OD1	616	A	GLN	NE2	3.07
101	C	TYR	OH	616	A	GLN	OE1	2.43
147	C	ARG	NH1	618	A	GLN	OE1	3.11
147	C	ARG	NH1	618	A	GLN	OE1	3.11
After Simulation								
DONOR				**ACCEPTOR**				
POS	**CHAIN**	**RES**	**ATOM**	**POS**	**CHAIN**	**RES**	**ATOM**	**Dd-a**
616	A	GLN	NE2	75	C	ASP	OD1	2.99
616	A	GLN	NE2	75	C	ASP	OD1	2.99
616	A	GLN	OE1	101	C	TYR	OH	2.5
616	A	GLN	OE1	101	C	TYR	OH	2.5
619	A	THR	OG1	99	C	GLU	OE2	2.85
634	A	HIS	ND1	168	C	GLN	NE2	2.78
75	C	ASP	OD1	616	A	GLN	NE2	2.99
75	C	ASP	OD1	616	A	GLN	NE2	2.99
101	C	TYR	OH	616	A	GLN	OE1	2.5
147	C	ARG	NH1	618	A	GLN	OE1	3
147	C	ARG	NH1	618	A	GLN	OE1	3
168	C	GLN	NE2	634	A	HIS	ND1	2.78
168	C	GLN	NE2	634	A	HIS	ND1	2.78
31	P	THR	OG1	370	A	SER	OG	2.91

Table 3.3.5: Protein-Protein Ionic Interactions of PSKR-Phytosulfokine-SERk1 complex before and after simulation.

Before Simulation					
Position	**Residue**	**Chain**	**Position**	**Residue**	**Chain**
514	ARG	A	68	GLU	C

574	GLU	A	62	HIS	C
After Simulation					
Position	**Residue**	**Chain**	**Position**	**Residue**	**Chain**
158	LYS	A	31	ASP	C
574	GLU	A	62	HIS	C

Table 3.3.6: Protein-Protein Aromatic interaction of PSKR-Phytosulfokine-SERk1 complex before and after simulation.

Before Simulation						
NO PROTEIN-PROTEIN AROMATIC-AROMATIC INTERACTIONS FOUND						
After Simulation						
Position	**Residue**	**Chain**	**Position**	**Residue**	**Chain**	**D(centroid-centroid)**
620	PHE	A	97	TYR	C	6.55

Table 3.3.7: Protein-Protein Cation-Pi interaction of PSKR-Phytosulfokine-SERk1 complex before and after simulation.

Before Simulation						
NO PROTEIN-PROTEIN CATION-PI INTERACTIONS FOUND						
After Simulation						
Position	**Residue**	**Chain**	**Position**	**Residue**	**Chain**	**D(cation-Pi)**
620	PHE	A	73	ARG	C	4.03

Table 3.3.8: Protein-Protein Hydrophobic Interaction of PSKR-SERk1 complex (Phytosulfokine absent) before and after simulation.

Before Simulation					
Position	**Residue**	**Chain**	**Position**	**Residue**	**Chain**
111	PHE	A	38	VAL	C
525	PRO	A	61	PHE	C
526	PRO	A	61	PHE	C
596	PHE	A	46	VAL	C
596	PHE	A	79	ALA	C
After Simulation					
Position	**Residue**	**Chain**	**Position**	**Residue**	**Chain**
111	PHE	A	38	VAL	C
525	PRO	A	61	PHE	C
526	PRO	A	61	PHE	C
596	PHE	A	46	VAL	C
596	PHE	A	76	LEU	C
596	PHE	A	79	ALA	C
621	PRO	A	97	TYR	C

Table 3.3.9: Hydrogen bond (main chain-side chain) of PSKR -SERk1 (Phytosulfokine absent) before and after simulation.

Before Simulation								
DONOR				**ACCEPTOR**				
POS	**CHAIN**	**RES**	**ATOM**	**POS**	**CHAIN**	**RES**	**ATOM**	**Dd-a**
87	A	LYS	NZ	38	C	VAL	O	3.28
595	A	SER	OG	77	C	GLY	O	2.97
62	C	HIS	N	574	A	GLU	OE2	2.83
73	C	ARG	NH1	619	A	THR	O	3.01
73	C	ARG	NH1	619	A	THR	O	3.01
After Simulation								

DONOR				ACCEPTOR				
POS	**CHAIN**	**RES**	**ATOM**	**POS**	**CHAIN**	**RES**	**ATOM**	**Dd-a**
87	A	LYS	NZ	38	C	VAL	O	2.94
514	A	ARG	NE	67	C	ASN	O	3.46
514	A	ARG	NH1	67	C	ASN	O	3.42
514	A	ARG	NH1	67	C	ASN	O	3.42
514	A	ARG	NH2	67	C	ASN	O	3.19
514	A	ARG	NH2	67	C	ASN	O	3.19
615	A	GLY	N	123	C	ASP	OD1	3.41
62	C	HIS	N	574	A	GLU	OE1	3.17
62	C	HIS	N	574	A	GLU	OE2	3.43
97	C	TYR	OH	619	A	THR	O	2.63

Table 3.3.10: Hydrogen bond (side chain-side chain) of PSKR -SERk1 (Phytosulfokine absent) before and after simulation.

Before Simulation

DONOR				ACCEPTOR				
POS	**CHAIN**	**RES**	**ATOM**	**POS**	**CHAIN**	**RES**	**ATOM**	**Dd-a**
616	A	GLN	NE2	75	C	ASP	OD1	3.07
616	A	GLN	NE2	75	C	ASP	OD1	3.07
616	A	GLN	OE1	101	C	TYR	OH	2.43
616	A	GLN	OE1	101	C	TYR	OH	2.43
75	C	ASP	OD1	616	A	GLN	NE2	3.07
75	C	ASP	OD1	616	A	GLN	NE2	3.07
101	C	TYR	OH	616	A	GLN	OE1	2.43
147	C	ARG	NH1	618	A	GLN	OE1	3.11
147	C	ARG	NH1	618	A	GLN	OE1	3.11

After Simulation

DONOR				ACCEPTOR				
POS	**CHAIN**	**RES**	**ATOM**	**POS**	**CHAIN**	**RES**	**ATOM**	**Dd-a**
616	A	GLN	NE2	75	C	ASP	OD1	2.69
616	A	GLN	NE2	75	C	ASP	OD1	2.69
616	A	GLN	OE1	101	C	TYR	OH	2.94
616	A	GLN	OE1	101	C	TYR	OH	2.94
619	A	THR	OG1	99	C	GLU	OE2	2.8
75	C	ASP	OD1	616	A	GLN	NE2	2.69
75	C	ASP	OD1	616	A	GLN	NE2	2.69
101	C	TYR	OH	616	A	GLN	OE1	2.94
147	C	ARG	NH1	618	A	GLN	OE1	3.13
147	C	ARG	NH1	618	A	GLN	OE1	3.13
147	C	ARG	NH2	618	A	GLN	OE1	2.93
147	C	ARG	NH2	618	A	GLN	OE1	2.93

Table 3.3.11: Protein-Protein ionic interaction of PSKR- SERk1 (Phytosulfokine absent) before and after simulation.

Before Simulation					
Position	**Residue**	**Chain**	**Position**	**Residue**	**Chain**
514	ARG	A	68	GLU	C
574	GLU	A	62	HIS	C
After Simulation					
Position	**Residue**	**Chain**	**Position**	**Residue**	**Chain**
158	LYS	A	31	ASP	C
574	GLU	A	62	HIS	C

Table 3.3.12: Protein-Protein cation-pi interaction of PSKR- SERk1 (Phytosulfokine absent) before and after simulation.

Before Simulation						
NO PROTEIN-PROTEIN CATION-PI INTERACTIONS FOUND						
After Simulation						
Position	**Residue**	**Chain**	**Position**	**Residue**	**Chain**	**D(cation-Pi)**
620	PHE	A	73	ARG	B	3.88

Table 3.3.13: Protein-Protein Hydrophobic Interaction of PSKR-Phytosulfokine complex (SERk1 absent) before and after simulation.

Before Simulation					
Position	**Residue**	**Chain**	**Position**	**Residue**	**Chain**
421	VAL	A	29	ILE	P
443	LEU	A	29	ILE	P
467	TYR	A	29	ILE	P
505	PHE	A	29	ILE	P
507	MET	A	29	ILE	P
524	PHE	A	29	ILE	P
After Simulation					
Position	**Residue**	**Chain**	**Position**	**Residue**	**Chain**
507	MET	A	29	ILE	P

Table 3.3.14: Protein-Protein Main Chain-Main Chain Hydrogen Bonds of PSKR-Phytosulfokine complex (SERk1 absent) before and after simulation.

Before Simulation								
DONOR				**ACCEPTOR**				
POS	**CHAIN**	**RES**	**ATOM**	**POS**	**CHAIN**	**RES**	**ATOM**	**Dd-a**
325	A	THR	N	32	P	GLN	O	3.46

After Simulation								
DONOR				ACCEPTOR				
POS	**CHAIN**	**RES**	**ATOM**	**POS**	**CHAIN**	**RES**	**ATOM**	**Dd-a**
31	P	THR	N	506	A	PHE	O	3.43

Table 3.3.15: Protein-Protein Main Chain-Side Chain Hydrogen Bonds of PSKR-Phytosulfokine complex (SERk1 absent) before and after simulation.

Before Simulation								
DONOR				ACCEPTOR				
POS	**CHAIN**	**RES**	**ATOM**	**POS**	**CHAIN**	**RES**	**ATOM**	**Dd-a**
325	A	THR	OG1	32	P	GLN	O	2.61
346	A	ASN	ND2	32	P	GLN	OXT	2.9
346	A	ASN	ND2	32	P	GLN	OXT	2.9
398	A	THR	OG1	29	P	ILE	O	2.73
29	P	ILE	N	445	A	ASP	OD2	2.95
31	P	THR	N	372	A	SER	OG	3.2
After Simulation								
DONOR				ACCEPTOR				
POS	**CHAIN**	**RES**	**ATOM**	**POS**	**CHAIN**	**RES**	**ATOM**	**Dd-a**
372	A	SER	OG	29	P	ILE	O	2.65
372	A	SER	OG	31	P	THR	O	3.15
506	A	PHE	N	31	P	THR	OG1	2.96

Table 3.3.16: Protein-Protein Side Chain-Side Chain Hydrogen Bonds of PSKR-Phytosulfokine complex (SERk1 absent) before and after simulation.

Before Simulation								
DONOR				ACCEPTOR				
POS	**CHAIN**	**RES**	**ATOM**	**POS**	**CHAIN**	**RES**	**ATOM**	**Dd-a**
349	A	ARG	NH1	32	P	GLN	OE1	3.16

349	A	ARG	NH1	32	P	GLN	OE1	3.16

After Simulation

NO PROTEIN-PROTEIN SIDE CHAIN-SIDE CHAIN HYDROGEN BONDS FOUND

Table 3.3.17: Summary of interactions among PSKR, Phytosulfokine and SERk1 before and after simulation.

Complex	Inter. Bet.	H-Bond		Hydrophobic Interaction		Ionic Interaction		Cation - Pi Interaction		Aromatic - Aromatic Interaction		Aromatic - Sulphur Interaction	
		B. MD	*A. MD*	*B. MD*	*A. MD*	*B. MD*	*A. MD*	*B. MD*	*A. MD*	*B. MD*	*A. MD*	*B. MD*	*A. MD*
PSKR+ phytosulfokine+ SERk1	*PSKR+ Phytosulfokine*	9	2	6	5	0	0	0	0	0	0	0	0
	PSKR+ SERk1	14	24	5	5	2	2	0	1	0	1	0	0
	Phytosulfokine + SERk1	0	0	0	0	0	0	0	0	0	0	0	0
PSKR+ SERk1	*PSKR+ SERk1*	14	22	5	7	2	2	0	1	0	0	0	0
PSKR+ phytosulfokine	*PSKR+ Phytosulfokine*	9	4	6	1	0	0	0	0	0	0	0	0

3.4 Root Mean Square Deviation (RMSD)

Throughout the cases of deviations, the consistency of the MD simulation was evaluated by observing Root mean square deviation (RMSD). As a function of the time, the time shift of the RMSDs of PSKR, phytosulfokine and SERK1 (backbone only) is monitored. Particularly, the RMSDs for PSKR, phytosulfokine and SERK1 in the three simulated frameworks are shown in Fig 3.4.1. In divergent simulated schemes, the backbone of three proteins exhibited variable RMSD. For PSKR, phytosulfokine and SERK1, a balance of 20ns is desired. This offers optimum deviation at 17ns and 14ns, which are 0.57nm and 0.49nm, until 20ns of the time span. While the time graph goes slightly down at 11ns(0.22nm) between this span of time after equilibrium, it moves firmly forward with a standard deviation (SD) of 0.40nm. It has a fairly constant position of 20 ns and deviated before the end of the simulation from 0.35nm to 0.45nm. On the counter, when SERK1 is absent in the complex, the PSKR and phytosulfokine complex variations are not as consistent as they were in the previous. Rather, the graph reveals rigidity at the very beginning of the simulation process. After 15ns, indeed, the highest deviation continues to remain, also at 16ns it deviates at 0.83nm, which is regarded as the highest in that order. Throughout this case, instability too is observed from 16ns to 20ns since it shows some high RMSDs such as 0.80nm to 0.83nm between this period. PSKR and SERK1's RMSD are interpreted in the similar method. Like earlier, the complex's primary phase is balanced and illustrates equilibrium. It deviates to 0.36nm at 11ns and dramatically rises to 0.56nm after 14ns, while the RMSD poses slight uniformity with a standard deviation of 0.35nm from 20ns to 23ns of the simulation, but discontinues prior to the end of simulation. As seen prior, an unstable deviation is similarly defined that PSKR and SEKR1 RMSD without phytosulfokine also demonstrate instability in the context of PSKR and phytosulfokine RMSD lacking SERK1. As it is noted, when SERK1 is present in the PSKR and phytosulfokine RMSD complex, it shows 20ns stability, but in this case it is unstable from 24ns till the end of the simulation time apparently. Throughout all three scenarios, it is recognized that PSKR, phytosulfokine and SERK1 RMSD have greater stability when all of them are inside the complex and engage with each other. Excluding SERK1, PSKR RMSD and phytosulfokine deviate more and further some other scenario is shown to be unstable. SERK1 must therefore be present for the interaction of PSKR with phytosulfokine.

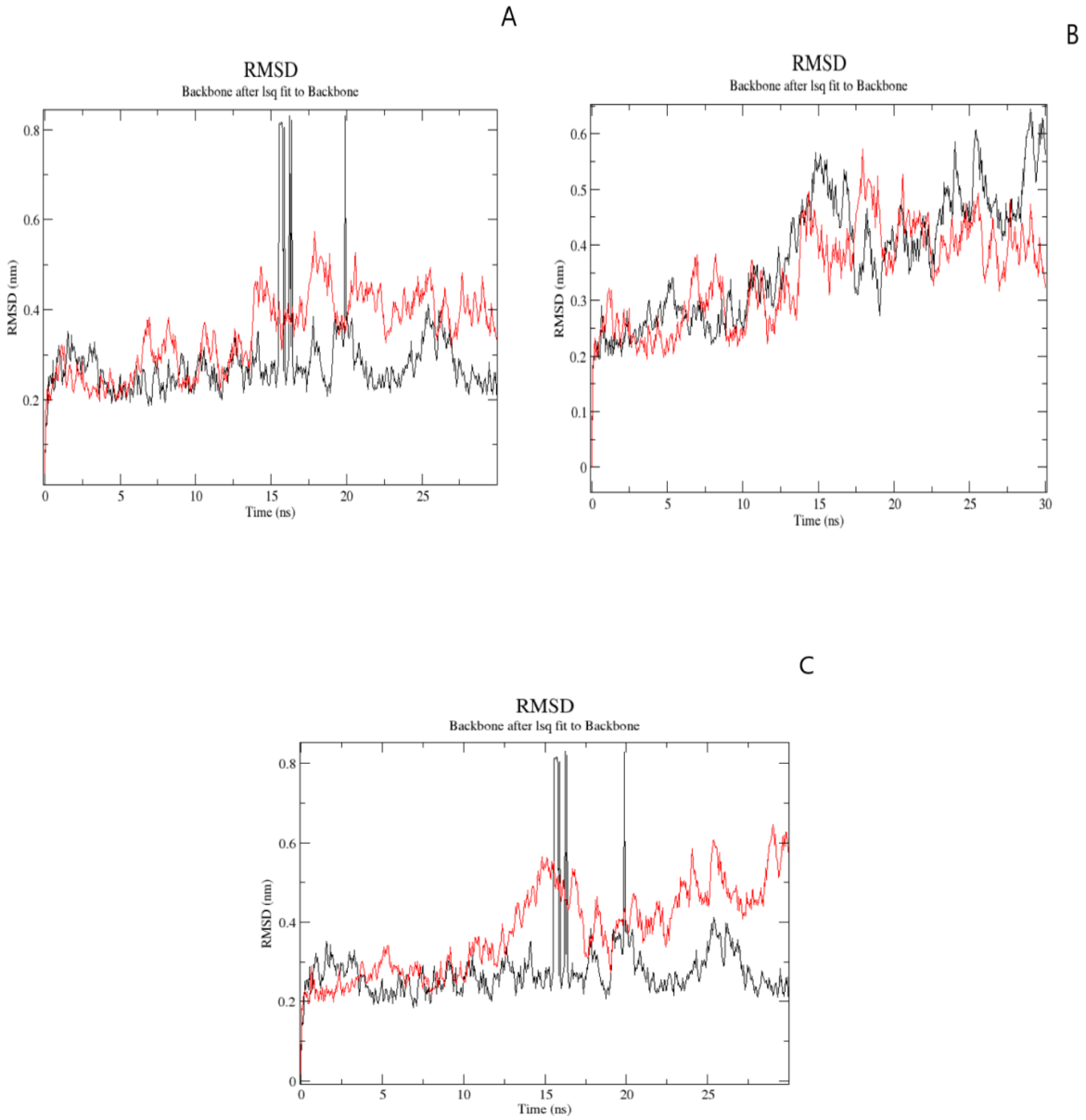

Fig 3.4.1: (A) RMSD value of PSKR and Phytosulfokine from 30ns MD trajectories. RMSD of PSKR and Phytosulfokine when SERk1 is present in the complex (Black). RMSD of PSKR and Phytosulfokine when SERk1 is absent in the complex (Red). **(B)** RMSD value of PSKR and SERk1 from 30ns MD trajectories. RMSD of PSKR and SERk1 when Phytosulfokine is present in the complex (Black). RMSD of PSKR and SERk1 in the absence of Phytosulfokine (Red). **(C)** RMSD value of Phytosulfokine and SERk1 from 30ns MD trajectories. RMSD of

Phytosulfokine and SERk1 at the presence of PSKR (Red). RMSD value of Phytosulfokine and SERk1 in the absence of PSKR inside the complex (Black).

3.5 Radius of Gyration

Radius of gyration (Rg) values is measured to evaluate the compactness of all the schemes. In addition, contrasts sharply with the PSKR- phytosulfokine-SERK1 complex and the PSKR-SERK1 complex, the Rg of the PSKR- Phytosulfokine complex has further fluctuated. As the PSKR- Phytosulfokine complex stretches to the peak value of about 3.16 nm during the first 14 ns and then goes down and hits the lowest value of about 2.90 nm near the 20 ns level, this pattern is most noticeable in the 20 ns of the simulation. In this time frame, the graph remains comparatively consistent with the PSKR- phytosulfokine-SERK1 complex; Nonetheless, at around 18 ns and 9 ns, it also hits its peak (around 3.35 nm) and lowest (around 3.10 nm) spikes. Although it gives the lowest value of 3.04nm after 15ns in the PSKR-SERK1 complex at a beginning period of the simulation (4ns), it increases to 3.3nm and establishes firmness. Numerous instabilities usually happen in PSKR- phytosulfokine complexes. Though it grows to 3.16nm at 20ns, it declines to 2.98nm at 22ns after that. A further modifying structure, which is persistent with higher variations in the PSKR-SERK1 complex and PSKR- phytosulfokine complex, reflects further variations in the Rg values; Since the proteins are likely to uncoil and recoil often spontaneously. Conversely, as SERK1 interacts in a single complex with both PSKR and phytosulfokine, it is confined in phase but also less susceptible to uncoil, likely to result in a less fluctuating graph.

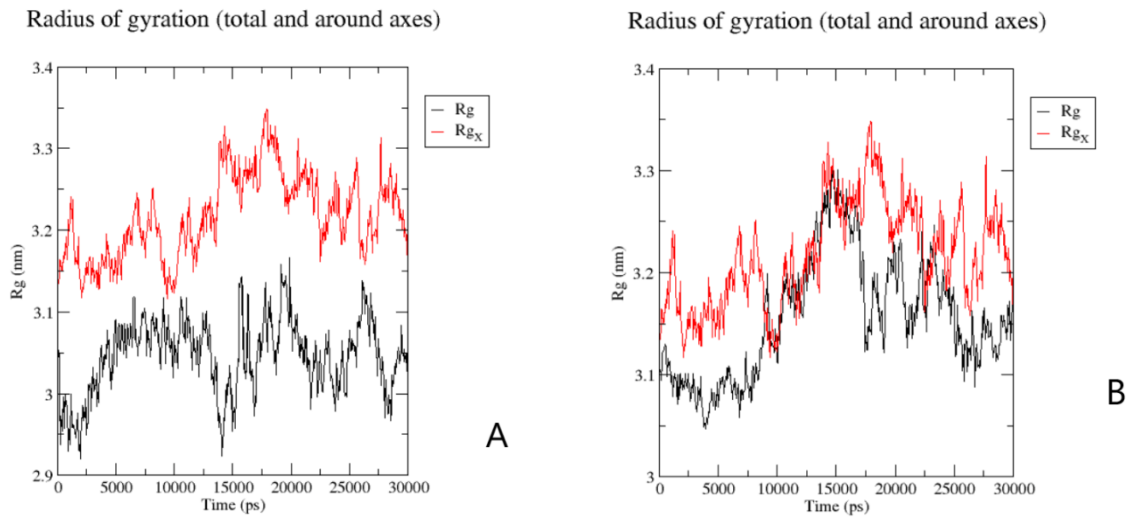

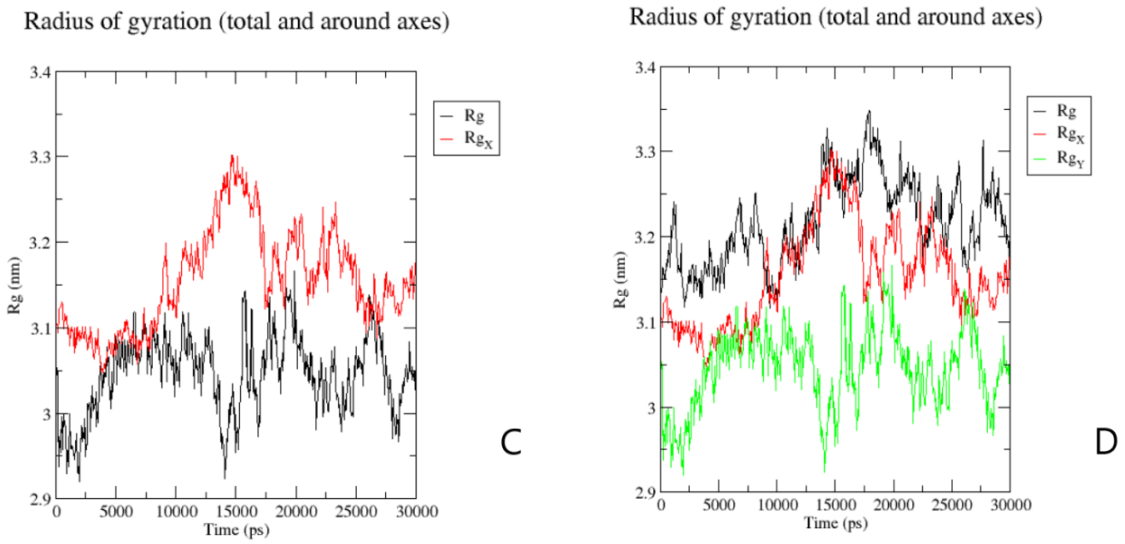

Fig 3.5.1: (A) Rg value of PSKR and Phytosulfokine from 30ns MD trajectories. Rg of PSKR and Phytosulfokine when SERk1 is present in the complex (Black). Rg of PSKR and Phytosulfokine when SERk1 is absent in the complex (Red). **(B)** Rg value of PSKR and SERk1 from 30ns MD trajectories. Rg of PSKR and SERk1 when Phytosulfokine is present in the complex (Black). Rg of PSKR and SERk1 in the absence of Phytosulfokine (Red). **(C)** Rg value of Phytosulfokine and SERk1 from 30ns MD trajectories. Rg of Phytosulfokine and SERk1 at the presence of PSKR (Black). Rg value of Phytosulfokine and SERk1 in the absence of PSKR inside the complex (Red). **(D)** Rg value of all complex with the addition of PSKR only (Green).

3.6 Solvent Accessible Surface Area (SASA)

Solvent assessable surface areas (SASA) were also assessed and the PSKR- phytosulfokine-SERK1 complex was found to be slightly higher than the PSKR- phytosulfokine complex, demonstrating a steady mean value of approximately 345 $nm^{2.}$ The PSKR-SERK1 complex, in comparison, had a slightly higher mean value of approximately 350 nm2. In addition, the PSKR- phytosulfokine complex's SASA value is 275 nm2, which is quite small.

It was anticipated that the interaction of phytosulfokine with the territories of the PSKR LRR and also the interaction of PSKR, phytosulfokine and SERK1 greatly increased the surface area of the complex which could be accessible for water (in this case, the solvent).

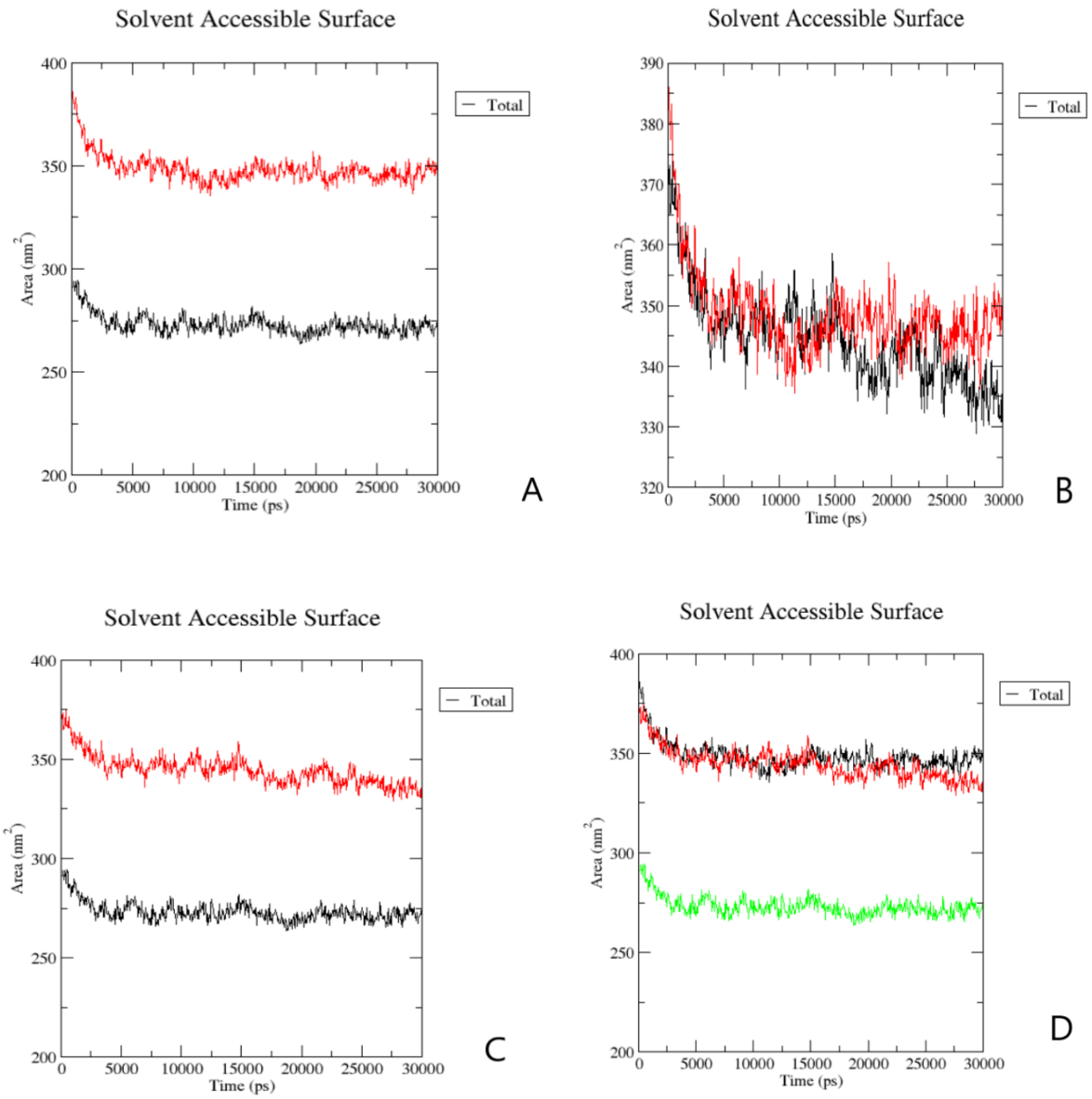

Fig 3.6.1: (A) SASA value of PSKR and Phytosulfokine from 30ns MD trajectories. SASA of PSKR and Phytosulfokine when SERk1 is present in the complex (Black). SASA of PSKR and Phytosulfokine when SERk1 is absent in the complex (Red). **(B)** SASA value of PSKR and SERk1 from 30ns MD trajectories. SASA of PSKR and SERk1 when Phytosulfokine is present in the complex (Black). SASA of PSKR and SERk1 in the absence of Phytosulfokine (Red). **(C)** SASA value of Phytosulfokine and SERk1 from 30ns MD trajectories. SASA of Phytosulfokine and SERk1 at the presence of PSKR (Black). SASA value of Phytosulfokine

and SERk1 in the absence of PSKR inside the complex (Red). **(D)** SASA value of all complex with the addition of PSKR only (Green).

3.7 Discussion

The computational assessment of a plant PRR and the correlation between PRR-RLK PSKR and PAMP Phytosulfokine and Co-receptor SERk1 was described and evaluated. Divergent systematic approaches used in this analysis to explain *Arabidopsis thaliana* Pattern Triggered Immunity (PTI) towards Phytosulfokine by using the domain of PSKR LRR.

In addition, a detailed review of Phytosulfokine and PSKR LRR domain interactions reveals that Arg300 from PSKR also interacts favorably with phytosulfokine during the absence of SERK1 in the complex yet, Other residues in the company of SERK1 reveal favorable interaction. From phytosulfokine interaction it is found that, Thr31 is more so favourable in SERK1's existence. Gln32, conversely, offers favourable interaction in the nonexistence of SERk1. Both the residues create more favorable conditions for PSKR and SERK1 interaction while phytosulfokine remains in the complex. Nonetheless, when phytosulfokine is absent in the complex, Asp42 and Glu80 from SERK1 are more favorable. There is no noteworthy binding energy seen in the absence of Phytosulfokine. Throughout the presence of Phytosulfokine, the interaction among PSKR and SERK1 goes to a persistent form afterwards through RMSF and RMSD inspections, a clear simulation period and even salient residues are defined in the course of this time as very low fluctuations. From the analysis of H-bond and protein interaction calculation (PIC) data, it is shown that previously explained favorable residues have a variety of interactions besides hydrogen bond. Cross search between formerly studied crystallographic structures and the PSKR-Phytosulfokine-SERk1 complex is supervised for additional observations. Some processes are naturally followed in order to interact with LRR-RKs and peptide hormones. In specific, peptidyl hormone residues interact with the internal component of LRR in a complete conformation. [109, 110]SERK1's Asp31 supplies atoms to PSKR's Lys158 to incorporate ionic contact. In addition, phytosulfokine's Thr31 also constructs the side chain-side chain in the proximity of SERK1 via its Ser370 and Connection of the main chain side chain via Phe506 in the exclusion of SERK1. LRR-RK ectodomains ultimately perform the function of regulators that assess the optimal distance of a bioactive peptide by connecting with the peptide hormones' somewhat more precise mature C terminus.

In addition to this, as it has been observed that, Phytosulfokine is not explicitly engaged throughout the connection with PSKR-SERK1, yet adjusts the PSKR island domain for SERK's liaison by promoting PSKR-SERK1 heterodimerization. It also offers a correlation between both the detection of Phytosulfokine and initial intracellular signaling that further support for the hypothesis of dimerization. Thus Pathogen-associated molecular pattern (PAMP)-triggered immunity supervised in a negative way by the phytosulfokine signaling. Moreover, Phytosulfokine-enhanced heterodimerization of PSKR-SERK1 can also make a significant contribution to the transphosphorylation of both receptor kinases (RK). So, it can be said undoubtedly, PSKR1 kinase function is vital for Phytosulfokine-induced plant development in Arabidopsis. In particular, it can be hypothesized that a mutation at those positions of PSKR's LRR-RK can substantially affect the competence of plants to detect the PAMP.

Chapter 4

Conclusions and Recommendations

4.1 Conclusions

Based on the study of 30ns of PSKR, Phytosulfokine and SERk1 complex trajectories applying RMSD, RMSF, H-bond, PIC and MM/PBSA, it does seem that co-receptor SERk1 must be subsist within the complex for the immune response against Phytosulfokine. Even though it is discovered from 30ns trajectories RMSD that after 30ns the entire complex appears to be stable, but if the simulation span of time is prolonged to 50ns or 100ns, more rigidity could be identified. In addition, the pivotal residues identified with MM/PBSA is measured from trajectories of 30ns. There have been significant differences observed both from H-bond and PIC findings after 30ns simulation in various forms of interaction adjacent to H-bond than before the simulation. The prolonged time of simulation would show which kinds of interactions are more essential and which interactions are less significant. However, from 30ns trajectories, as it is identified for immune responsiveness from PSKR co-receptor plays a noteworthy part, therefore it can be presumed that after the development of the simulation period it will persist to be uniform.

4.2 Recommendations for Future Works

This study can be further advanced by acquiring certain standard for instance:

1. This research can be enhanced by operating the molecular dynamics (MD) simulation for considerably longer (50 ns or 100 ns), this would permit further particular and decisive outcomes from the research. More comprehension of protein character can be constructed.

2. This research might be advantageous for the interlinkages of PSKR LRR along with additional mutated PAMPs in plant Arabidopsis thaliana. Fundamental interaction of PRR-PAMP complex as well as the engagement of mutated co-receptor can demonstrate in which way mutant molecule can be able to cause a modification in specific residues and impacts in their interactions that results in pattern triggered immunity (PTI).

3. MM/PBSA is a post-processing approach through which the free energy of a condition is decided from the interior energy (MM) of the residues and its linkage with an comprehensible

representation of solvent (PBSA). FEP, parallel to other free energy estimation (TI, BAR, and so forth) evaluates free energy dissimilarities of a provided scheme under a substitute Hamiltonian (for example one whose cooperation's are ascended by a lambda factor). Approximation that occupies FEP are significantly expensive than MM/PBSA, which operates a single trajectory, run utilizing common MD. whereas additional free energy methods, same as TI and BAR, are more accurate than MM/PBSA, they are in a restrictive manner high cost for bigger solutes like macromolecules. For evaluating restricting free energies whereby, the ligand to be uncoupled is small-scale. For solvation free energies of proteins, DNA, and things of that sort, MM/PBSA is appropriately precise and submits a calculated range from the tremendous expense that would appear from using decoupling methods.

References

1. Boller, T. and G.J.A.r.o.p.b. Felix, *A renaissance of elicitors: perception of microbe-associated molecular patterns and danger signals by pattern-recognition receptors.* 2009. 60: p. 379-406.
2. Boller, T. and S.Y.J.S. He, *Innate immunity in plants: an arms race between pattern recognition receptors in plants and effectors in microbial pathogens.* 2009. 324(5928): p. 742-744.
3. Chisholm, S.T., et al., *Host-microbe interactions: shaping the evolution of the plant immune response.* 2006. **124**(4): p. 803-814.
4. Hohmann, U., K. Lau, and M.J.A.r.o.p.b. Hothorn, *The structural basis of ligand perception and signal activation by receptor kinases.* 2017. **68**: p. 109-137.
5. Jones, J.D. and J.L.J.n. Dangl, *The plant immune system.* 2006. **444**(7117): p. 323-329.
6. Zipfel, C.J.T.i.i., *Plant pattern-recognition receptors.* 2014. **35**(7): p. 345-351.
7. Ting, J.P. and B.K.J.A.R.I. Davis, *CATERPILLER: a novel gene family important in immunity, cell death, and diseases.* 2005. **23**: p. 387-414.
8. Kaul, S., et al., *Analysis of the genome sequence of the flowering plant Arabidopsis thaliana.* 2000. **408**(6814): p. 796-815.
9. Meyerowitz, E.M. and C.R. Somerville, *Arabidopsis*. 1994: Cold Spring Harbor Laboratory Press.
10. Meinke, D.W., et al., *Arabidopsis thaliana: a model plant for genome analysis.* 1998. **282**(5389): p. 662-682.
11. Feldmann, K.A. and S.A.J.A.i.B.R. Goff, *The first plant genome sequence—Arabidopsis thaliana.* 2014. **69**: p. 91-117.
12. Sparrow, A., H. Price, and A. Underbrink. *A survey of DNA content per cell and per chromosome of prokaryotic and eukaryotic organisms: some evolutionary considerations*. in *Brookhaven symposia in biology*. 1972.
13. Sparrow, A.H. and J.P.J.S. Miksche, *Correlation of nuclear volume and DNA content with higher plant tolerance to chronic radiation.* 1961. **134**(3474): p. 282-283.
14. Lin, X., et al., *Sequence and analysis of chromosome 2 of the plant Arabidopsis thaliana.* 1999. **402**(6763): p. 761-768.
15. Mayer, K., et al., *Sequence and analysis of chromosome 4 of the plant Arabidopsis thaliana.* 1999. **402**(6763): p. 769-777.

16. Theologis, A., et al., *Sequence and analysis of chromosome 1 of the plant Arabidopsis thaliana.* 2000. **408**(6814): p. 816-820.
17. Meyerowitz, E.M.J.P.p., *Prehistory and history of Arabidopsis research.* 2001. **125**(1): p. 15-19.
18. Yanofsky, M.F., et al., *The protein encoded by the Arabidopsis homeotic gene agamous resembles transcription factors.* 1990. **346**(6279): p. 35-39.
19. Laibach, F., *Zur Frage nach der Individualitat der Chromosomen im Pflanzenreich*. 1907, Bonn.
20. Ezhova, T.J.G., *Arabidopsis thaliana (L.) Heynh. as a model object for studying genetic control of morphogenesis.* 1999. **35**(11): p. 1522-1537.
21. Frey, K.J., R.H. Burris, and B. Griffing, *Historical Perspectives in Plant Sciences*. 2002: Purdue University Press.
22. Laibach, F.J.B.A., *Arabidopsis thaliana (L.) Heynh. als Objekt für genetische und entwicklungsphysiologische Untersuchungen.* 1943. **44**: p. 439-455.
23. Rédei, G.P.J.A.r.o.g., *Arabidopsis as a genetic tool.* 1975. **9**(1): p. 111-127.
24. Tsuda, K. and F.J.C.o.i.p.b. Katagiri, *Comparing signaling mechanisms engaged in pattern-triggered and effector-triggered immunity.* 2010. **13**(4): p. 459-465.
25. Tsuda, K., et al., *Network properties of robust immunity in plants.* 2009. **5**(12): p. e1000772.
26. Block, A., et al., *Phytopathogen type III effector weaponry and their plant targets.* 2008. **11**(4): p. 396-403.
27. Cunnac, S., M. Lindeberg, and A.J.C.o.i.m. Collmer, *Pseudomonas syringae type III secretion system effectors: repertoires in search of functions.* 2009. **12**(1): p. 53-60.
28. Göhre, V. and S.J.A.r.o.p. Robatzek, *Breaking the barriers: microbial effector molecules subvert plant immunity.* 2008. **46**: p. 189-215.
29. Böhm, H., et al., *Immune receptor complexes at the plant cell surface.* 2014. **20**: p. 47-54.
30. Ranf, S.J.C.O.i.P.B., *Sensing of molecular patterns through cell surface immune receptors.* 2017. **38**: p. 68-77.
31. Xin, X.-F., et al., *Bacteria establish an aqueous living space in plants crucial for virulence.* 2016. **539**(7630): p. 524-529.
32. Rosebrock, T.R., et al., *A bacterial E3 ubiquitin ligase targets a host protein kinase to disrupt plant immunity.* 2007. **448**(7151): p. 370-374.

33. Collier, S.M. and P.J.T.i.p.s. Moffett, *NB-LRRs work a "bait and switch" on pathogens.* 2009. **14**(10): p. 521-529.
34. Mishra, A.K., K. Sharma, and R.S.J.J.o.p.i. Misra, *Elicitor recognition, signal transduction and induced resistance in plants.* 2012. **7**(2): p. 95-120.
35. Kaufmann, C., M. Motzkus, and M.J.J.o.e.b. Sauter, *Phosphorylation of the phytosulfokine peptide receptor PSKR1 controls receptor activity.* 2017. **68**(7): p. 1411-1423.
36. Pan, S., et al., *Bio-active peptides: Role in plant growth and defense*, in *Natural Bio-active Compounds*. 2019, Springer. p. 1-29.
37. Wang, J., et al., *Allosteric receptor activation by the plant peptide hormone phytosulfokine.* 2015. **525**(7568): p. 265-268.
38. Hanks, S.K. and T.J.T.F.j. Hunter, *The eukaryotic protein kinase superfamily: kinase (catalytic) domain structure and classification 1.* 1995. **9**(8): p. 576-596.
39. Hanks, S.K., A.M. Quinn, and T.J.S. Hunter, *The protein kinase family: conserved features and deduced phylogeny of the catalytic domains.* 1988. **241**(4861): p. 42-52.
40. Akira, S. and K.J.N.r.i. Takeda, *Toll-like receptor signalling.* 2004. **4**(7): p. 499-511.
41. Medzhitov, R. and C.A.J.S. Janeway, *Decoding the patterns of self and nonself by the innate immune system.* 2002. **296**(5566): p. 298-300.
42. Nürnberger, T., et al., *Innate immunity in plants and animals: striking similarities and obvious differences.* 2004. **198**(1): p. 249-266.
43. Zipfel, C., et al., *Perception of the bacterial PAMP EF-Tu by the receptor EFR restricts Agrobacterium-mediated transformation.* 2006. **125**(4): p. 749-760.
44. Ausubel, F.M.J.N.i., *Are innate immune signaling pathways in plants and animals conserved?* 2005. **6**(10): p. 973-979.
45. Zipfel, C. and G.J.C.o.i.p.b. Felix, *Plants and animals: a different taste for microbes?* 2005. **8**(4): p. 353-360.
46. Espinosa, A. and J.R.J.C.m. Alfano, *Disabling surveillance: bacterial type III secretion system effectors that suppress innate immunity.* 2004. **6**(11): p. 1027-1040.
47. Kim, M.G., et al., *Two Pseudomonas syringae type III effectors inhibit RIN4-regulated basal defense in Arabidopsis.* 2005. **121**(5): p. 749-759.
48. Nomura, K., M. Melotto, and S.-Y.J.C.o.i.p.b. He, *Suppression of host defense in compatible plant–Pseudomonas syringae interactions.* 2005. **8**(4): p. 361-368.

49. Jones, D.A. and D.J.C.o.i.i. Takemoto, *Plant innate immunity–direct and indirect recognition of general and specific pathogen-associated molecules.* 2004. **16**(1): p. 48-62.
50. Nimchuk, Z., et al., *Recognition and response in the plant immune system.* 2003. **37**(1): p. 579-609.
51. Matsubayashi, Y., et al., *Disruption and overexpression of Arabidopsis phytosulfokine receptor gene affects cellular longevity and potential for growth.* 2006. **142**(1): p. 45-53.
52. Amano, Y., et al., *Tyrosine-sulfated glycopeptide involved in cellular proliferation and expansion in Arabidopsis.* 2007. **104**(46): p. 18333-18338.
53. Albrecht, C., et al., *The Arabidopsis thaliana SOMATIC EMBRYOGENESIS RECEPTOR-LIKE KINASES1 and 2 control male sporogenesis.* 2005. **17**(12): p. 3337-3349.
54. Hecht, V., et al., *The Arabidopsis SOMATIC EMBRYOGENESIS RECEPTOR KINASE 1 gene is expressed in developing ovules and embryos and enhances embryogenic competence in culture.* 2001. **127**(3): p. 803-816.
55. Karlova, R., et al., *The Arabidopsis somatic embryogenesis receptor-like kinase1 protein complex includes brassinosteroid-insensitive1.* 2006. **18**(3): p. 626-638.
56. Kwaaitaal, M., S. De Vries, and E.J.P. Russinova, *Arabidopsis thaliana Somatic Embryogenesis Receptor Kinase 1 protein is present in sporophytic and gametophytic cells and undergoes endocytosis.* 2005. **226**(1-2): p. 55-65.
57. Colcombet, J., et al., *Arabidopsis SOMATIC EMBRYOGENESIS RECEPTOR KINASES1 and 2 are essential for tapetum development and microspore maturation.* 2005. **17**(12): p. 3350-3361.
58. Shah, K., et al., *The Arabidopsis kinase-associated protein phosphatase controls internalization of the somatic embryogenesis receptor kinase 1.* 2002. **16**(13): p. 1707-1720.
59. Mosher, S., et al., *The tyrosine-sulfated peptide receptors PSKR1 and PSY1R modify the immunity of Arabidopsis to biotrophic and necrotrophic pathogens in an antagonistic manner.* 2013. **73**(3): p. 469-482.
60. Barnes, J.E.J.N., *Evolution of compact groups and the formation of elliptical galaxies.* 1989. **338**(6211): p. 123-126.
61. Karplus, M. and G.A.J.N. Petsko, *Molecular dynamics simulations in biology.* 1990. **347**(6294): p. 631-639.

62. Karplus, M. and J.A.J.N.s.b. McCammon, *Molecular dynamics simulations of biomolecules.* 2002. **9**(9): p. 646-652.
63. Becker, O.M., et al., *Computational biochemistry and biophysics*. 2001: Crc Press.
64. Tuckerman, M.E. and G.J.J.T.J.o.P.C.B. Martyna, *Understanding modern molecular dynamics: techniques and applications.* 2000. **104**(2): p. 159-178.
65. van Gunsteren, W.F., P.K. Weiner, and A.J. Wilkinson, *Computer simulation of biomolecular systems: theoretical and experimental applications*. Vol. 3. 2013: Springer Science & Business Media.
66. Allen, M.P.J.C.s.m.f.s.p.t.p., *Introduction to molecular dynamics simulation.* 2004. **23**(1): p. 1-28.
67. Bhaduri, A., et al., *Conserved spatially interacting motifs of protein superfamilies: application to fold recognition and function annotation of genome data.* 2004. **54**(4): p. 657-670.
68. Gromiha, M.M., S.J.P.i.b. Selvaraj, and m. biology, *Inter-residue interactions in protein folding and stability.* 2004. **86**(2): p. 235-277.
69. Krupa, A., G. Preethi, and N.J.J.o.m.b. Srinivasan, *Structural modes of stabilization of permissive phosphorylation sites in protein kinases: distinct strategies in Ser/Thr and Tyr kinases.* 2004. **339**(5): p. 1025-1039.
70. Reva, B.A., et al., *Recognition of protein structure on coarse lattices with residue-residue energy functions.* 1997. **10**(10): p. 1123-1130.
71. Russell, R.B. and G.J.J.J.o.m.b. Barton, *Structural features can be unconserved in proteins with similar folds: An analysis of side-chain to side-chain contacts secondary structure and accessibility.* 1994. **244**(3): p. 332-350.
72. Šali, A. and T.L.J.J.o.m.b. Blundell, *Comparative protein modelling by satisfaction of spatial restraints.* 1993. **234**(3): p. 779-815.
73. Shao, X. and N.V.J.N.A.R. Grishin, *Common fold in helix–hairpin–helix proteins.* 2000. **28**(14): p. 2643-2650.
74. Tina, K., R. Bhadra, and N.J.N.a.r. Srinivasan, *PIC: protein interactions calculator.* 2007. **35**(suppl_2): p. W473-W476.
75. Van Roey, P., et al., *Crystallographic and mutational studies of Mycobacterium tuberculosis recA mini-inteins suggest a pivotal role for a highly conserved aspartate residue.* 2007. **367**(1): p. 162-173.
76. Jones, S., J.M.J.P.i.b. Thornton, and m. biology, *Protein-protein interactions: a review of protein dimer structures.* 1995. **63**(1): p. 31-65.

77. Nooren, I.M. and J.M.J.T.E.j. Thornton, *Diversity of protein–protein interactions.* 2003. **22**(14): p. 3486-3492.
78. Ofran, Y. and B.J.J.o.m.b. Rost, *Analysing six types of protein–protein interfaces.* 2003. **325**(2): p. 377-387.
79. Rekha, N., et al., *Interaction interfaces of protein domains are not topologically equivalent across families within superfamilies: Implications for metabolic and signaling pathways.* 2005. **58**(2): p. 339-353.
80. Saha, R.P., et al., *Interaction geometry involving planar groups in protein–protein interfaces.* 2007. **67**(1): p. 84-97.
81. Bahadur, R.P., et al., *A dissection of specific and non-specific protein–protein interfaces.* 2004. **336**(4): p. 943-955.
82. De, S., et al., *Interaction preferences across protein-protein interfaces of obligatory and non-obligatory components are different.* 2005. **5**(1): p. 1-16.
83. Valdar, W.S. and J.M.J.J.o.m.b. Thornton, *Conservation helps to identify biologically relevant crystal contacts.* 2001. **313**(2): p. 399-416.
84. de Ruiter, A. and C.J.C.o.i.c.b. Oostenbrink, *Free energy calculations of protein–ligand interactions.* 2011. **15**(4): p. 547-552.
85. Genheden, S. and U.J.E.o.o.d.d. Ryde, *The MM/PBSA and MM/GBSA methods to estimate ligand-binding affinities.* 2015. **10**(5): p. 449-461.
86. Miller III, B.R., et al., *MMPBSA. py: an efficient program for end-state free energy calculations.* 2012. **8**(9): p. 3314-3321.
87. Foloppe, N. and R.J.C.m.c. Hubbard, *Towards predictive ligand design with free-energy based computational methods?* 2006. **13**(29): p. 3583-3608.
88. Homeyer, N. and H.J.M.i. Gohlke, *Free energy calculations by the molecular mechanics Poisson− Boltzmann surface area method.* 2012. **31**(2): p. 114-122.
89. Wang, J., T. Hou, and X.J.C.C.-A.D.D. Xu, *Recent advances in free energy calculations with a combination of molecular mechanics and continuum models.* 2006. **2**(3): p. 287-306.
90. Gohlke, H. and D.A.J.J.o.c.c. Case, *Converging free energy estimates: MM-PB (GB) SA studies on the protein–protein complex Ras–Raf.* 2004. **25**(2): p. 238-250.
91. Hou, T., et al., *Assessing the performance of the molecular mechanics/Poisson Boltzmann surface area and molecular mechanics/generalized Born surface area methods. II. The accuracy of ranking poses generated from docking.* 2011. **32**(5): p. 866-877.

92. Kumari, R., et al., *g_mmpbsa□ A GROMACS tool for high-throughput MM-PBSA calculations.* 2014. **54**(7): p. 1951-1962.
93. Moreira, I.S., P.A. Fernandes, and M.J.J.T.C.A. Ramos, *Unravelling Hot Spots: a comprehensive computational mutagenesis study.* 2007. **117**(1): p. 99-113.
94. Réblová, K., et al., *An RNA molecular switch: Intrinsic flexibility of 23S rRNA helices 40 and 68 5′-UAA/5′-GAN internal loops studied by molecular dynamics methods.* 2010. **6**(3): p. 910-929.
95. Sirin, S., et al., *A computational approach to enzyme design: predicting ω-aminotransferase catalytic activity using docking and MM-GBSA scoring.* 2014. **54**(8): p. 2334-2346.
96. Sun, H., et al., *Assessing the performance of MM/PBSA and MM/GBSA methods. 4. Accuracies of MM/PBSA and MM/GBSA methodologies evaluated by various simulation protocols using PDBbind data set.* 2014. **16**(31): p. 16719-16729.
97. Connolly, M.L.J.S., *Solvent-accessible surfaces of proteins and nucleic acids.* 1983. **221**(4612): p. 709-713.
98. Lee, B. and F.M.J.J.o.m.b. Richards, *The interpretation of protein structures: estimation of static accessibility.* 1971. **55**(3): p. 379-IN4.
99. Richards, F., *Annu. Rev. Biophys. Bioeng.* 1977.
100. Greer, J. and B.L.J.P.o.t.N.a.o.S. Bush, *Macromolecular shape and surface maps by solvent exclusion.* 1978. **75**(1): p. 303-307.
101. Jiang, F. and S.-H.J.J.o.m.b. Kim, *"Soft docking": matching of molecular surface cubes.* 1991. **219**(1): p. 79-102.
102. Shrake, A. and J.A.J.J.o.m.b. Rupley, *Environment and exposure to solvent of protein atoms. Lysozyme and insulin.* 1973. **79**(2): p. 351-371.
103. Creighton, T.E.J.C.o.i.s.b., *Stability of folded conformations: Current opinion in structural biology 1991, 1: 5–16.* 1991. **1**(1): p. 5-16.
104. Dill, K.A.J.B., *Dominant forces in protein folding.* 1990. **29**(31): p. 7133-7155.
105. Huggins, M.L.J.A.C.I.E.i.E., *50 Years of hydrogen bond theory.* 1971. **10**(3): p. 147-152.
106. McDonald, I.K. and J.M.J.J.o.m.b. Thornton, *Satisfying hydrogen bonding potential in proteins.* 1994. **238**(5): p. 777-793.
107. Van Der Spoel, D., et al., *GROMACS: fast, flexible, and free.* 2005. **26**(16): p. 1701-1718.

108. van der Spoel, D., P.J. Van Maaren, and H.J.J.T.J.o.c.p. Berendsen, *A systematic study of water models for molecular simulation: derivation of water models optimized for use with a reaction field.* 1998. **108**(24): p. 10220-10230.
109. Shinohara, H., et al., *Identification of three LRR-RKs involved in perception of root meristem growth factor in Arabidopsis.* 2016. **113**(14): p. 3897-3902.
110. Somssich, M., et al., *Real-time dynamics of peptide ligand–dependent receptor complex formation in planta.* 2015. **8**(388): p. ra76-ra76.

Appendixes

This research made use of a variety of bioinformatics resources, e.g.,

Tool	Purpose
Gromacs	MD simulation
Protein interactions calculator: PIC (online)	Residual bond identification
Chimera	Molecular visualization
g_mmpbsa	Binding free energy calculation
xmgrace	Graph generation and analysis